

DEFENCE



DÉFENSE

A One-Dimensional Mean Wind and Turbulence Model for a Uniform Urban Canopy

Eugene Yee
Defence Research Establishment Suffield

DISTRIBUTION STATEMENT A
Approved for Public Release
Distribution Unlimited

Technical Report
DRES TR 2000-071
October 2000



National
Defence

Défense
nationale

Canada

20010116 087

DTIC QUALITY INSPECTED 3

**A One-Dimensional Mean Wind and Turbulence
Model For a Uniform Urban Canopy**

Eugene Yee
Defence Research Establishment Suffield

Defence Research Establishment Suffield

Technical Report

DRES TR 2000-071

October 2000

Author

Eugene Yee

Approved by

Cam Boulet
H/CBDS

Approved for release by

Robert Herring
DRP Chair

Abstract

A fully analytical model for the prediction of the one-dimensional mean wind speed, kinematic shear stress, turbulence kinetic energy, and velocity variances in a horizontally homogeneous canopy is described. The basis of the model centers around an analytical solution obtained by Massman and Weil (Boundary-Layer Meteorology, **91**, pp. 81–107, 1999) for the turbulence kinetic energy derived from a particular form of a second-order closure model for canopy flows. Using this analytical model for the turbulence kinetic energy, it is shown how to derive analytical expressions for the within canopy velocity variances using two methods: namely, (1) equilibrium partitioning whereby the velocity variances are assumed to be proportional to the turbulence kinetic energy, with the proportionality constants the same as those at the canopy top; and, (2) algebraic stress model partitioning derived from an algebraic stress model version of an existing second-order closure model for flows proposed by Launder, Reece, and Rodi (Journal of Fluid Mechanics, **68**, pp. 537–566, 1975) that has been modified to include the effects on the turbulence of the extra physics arising from the interaction of the airflow with the obstacles in the array (viz., the form drag on the canopy elements, and the role of the momentum absorption over an extended volume of space on the turbulent motions within the canopy).

The predictions from the analytical model have been compared with some measurements of mean flow and turbulence statistics obtained in two urban canopies: namely, (1) Tombstone canopy; and, (2) arrays of regularly spaced cubical obstacles at various plan area indices. It is shown that the model is moderately successful at providing estimates of a number of important flow quantities; namely, mean wind speed and various turbulence statistics. Given the limited data that was available, it has not been possible to ascertain whether the algebraic stress model partitioning of the turbulence kinetic energy offers any significant advantages in the determination of the component velocity variances over the simpler equilibrium partitioning. With the testing of the analytical model against the urban canopy flows and its modest success, it is suggested that this analytical model for canopy flows can probably be applied unmodified to a wide range of canopies, both vegetative and urban.

This page intentionally left blank

Executive summary

Introduction: Incidents in Tokyo involving the use of chemical and biological warfare (CBW) agents by a terrorist organization have mobilized both military and public concerns on the use of these weapons against military and civilian populations in built-up or urban areas consisting of large groups of obstacles. In response to these increasing concerns, the prediction of the dispersion of CBW agents released within an urban area has recently become the subject for many investigations since information obtained from urban dispersion models will be used to form the basis on which government and military commanders (as well as other decision makers) will respond and act to mitigate the effects of a particular incident. Physically-based models such as Lagrangian Stochastic (LS) models exist for the prediction of plume or cloud dispersion in complex environments, and certainly can be applied to the problem of urban dispersion. The prediction of dispersion using LS models, which involves the calculation of the trajectories of a large number of tagged fluid particles representing the contaminant mass and the derivation of the ensemble-average concentration from the calculated particle distribution, is enticingly simple in concept and general in approach. However, for urban dispersion, LS models require to be provided information on the mean and statistical properties of the turbulent wind field within and above the urban canopy (e.g., mean wind speed, shear stress, velocity variances, etc.).

The mean flow and turbulence within and immediately above an urban canopy (wherein the atmospheric flow is influenced by the individual roughness elements or obstacles) possess a fully three-dimensional structure. Although the development of three-dimensional dynamical models of the mean flow and turbulence in simplified urban canopies consisting of large groups of regularly spaced obstacles is progressing, these models tend to require extensive computational resources. These flow models involve the solution of the conservation equations of mass, momentum, and energy, and the detailed information obtained from these models can be used to "drive" physically-based dispersion models to provide estimates of the contaminant concentrations. However, currently the computational demands of these three-dimensional models will preclude their use for emergency response situations which require the ability to generate a dispersion prediction in a time frame that will permit protective actions to be taken (i.e., time scales on the order of seconds to minutes). In view of this, we argue that for many practical applications it is convenient to consider spatial averages of the mean wind and turbulence within an urban canopy obtained by averaging horizontally the mean wind and turbulence statistics over an area that is much greater than the spacings between the individual roughness elements comprising the urban canopy. This provides a simplified one-dimensional mean wind and turbulence model for urban canopy flow whereby the flow statistics depend only on the height z . In this simplified description

of urban flow, the spatially-averaged mean wind and turbulence vary only with height, and the detailed three-dimensional description of flow and turbulence characteristics about the individual buildings is lost.

The primary objective of this report is to describe and test a simple, analytical one-dimensional model for the prediction of mean flow and turbulence within and above an urban canopy. This model was developed originally for vegetative canopies (e.g., forests, cereal crops, etc.), but will be applied here to urban canopies. While there are similarities between vegetative and urban canopies, there are enough important differences between these two types of canopies (e.g., characteristic density of roughness elements and their stiffness or ability to react to the drag forces) to require an independent evaluation of the model for the urban canopy application. It is hoped that this simple, analytical one-dimensional model for urban canopy flows can be used to provide useful input information on the statistics of the wind field required to drive LS models of urban dispersion.

Results: A fully analytical model for the prediction of the one-dimensional mean wind speed, kinematic shear stress, turbulence kinetic energy, and velocity variances in a horizontally homogeneous canopy is described. The basis of the model centers around an analytical solution obtained by Massman and Weil (Boundary-Layer Meteorology, **91**, pp. 81-107, 1999) for the turbulence kinetic energy derived from a particular form of a second-order closure model for canopy flows. Using this analytical model for the turbulence kinetic energy, it is shown how to derive analytical expressions for the within canopy velocity variances using two methods: namely, (1) equilibrium partitioning whereby the velocity variances are assumed to be proportional to the turbulence kinetic energy, with the proportionality constants the same as those at the canopy top; and, (2) algebraic stress model partitioning derived from an algebraic stress model version of an existing second-order closure model for flows proposed by Launder, Reece, and Rodi (Journal of Fluid Mechanics, **68**, pp. 537-566, 1975) that has been modified to include the effects on the turbulence of the extra physics arising from the interaction of the airflow with the obstacles in the array (viz., the form drag on the canopy elements, and the role of the momentum absorption over an extended volume of space on the turbulent motions within the canopy).

The predictions from the analytical model have been compared with some measurements of mean flow and turbulence statistics obtained in two urban canopies: namely, (1) Tombstone canopy; and, (2) arrays of regularly spaced cubical obstacles at various plan area indices. It is shown that the model is moderately successful at providing estimates of a number of important flow quantities; namely, mean wind speed and various turbulence statistics. Given the limited data that was available, it has not been possible to ascertain whether the

algebraic stress model partitioning of the turbulence kinetic energy offers any significant advantages in the determination of the component velocity variances over the simpler equilibrium partitioning. With the testing of the analytical model against the urban canopy flows and its modest success, it is suggested that this analytical model for canopy flows can probably be applied unmodified to a wide range of canopies, both vegetative and urban.

Significance and Future Plans: The one-dimensional analytical model for canopy flows considered in this report provides all the statistics of the wind field (mean wind speed, kinematic shear stress, velocity variances, and viscous dissipation rate) required as input to drive a physically-based model for the prediction of urban dispersion. These flow statistics can be calculated rapidly using the analytical model in comparison to the more computationally intensive second-order closure models for canopy flows. Taken as a whole, this simple canopy flow model can probably be used to "drive" a Lagrangian stochastic dispersion model for the prediction of dispersion of materials released within a canopy. The next logical step in this work would be to construct a Lagrangian stochastic model satisfying the well-mixed criterion that uses the simple analytical model to provide the input mean flow and turbulence quantities required.

Yee, E., 2000. A One-Dimensional Mean Wind and Turbulence Model for a Uniform Urban Canopy. DRES TR 2000-071, Defence Research Establishment Suffield.

This page intentionally left blank

Table of contents

Abstract	i
Executive summary	iii
Table of contents	vii
List of figures	ix
Introduction	1
Model for mean wind field and shear stress	3
Model for the TKE and velocity variances	7
Parameterizations for model inputs	13
Results	17
Conclusions	21
References	23

This page intentionally left blank

List of Figures

Figure 1. Comparison of the observed profile of the mean wind speed (open squares) in the Tombstone canopy with model predictions.....	27
Figure 2. Comparison of the observed profile of the kinematic shear stress (open squares) in the Tombstone canopy with model predictions.....	28
Figure 3. Comparison of the observed profile of turbulence kinetic energy (open squares) in the Tombstone canopy with model predictions.....	29
Figure 4. Comparison of the observed profile of streamwise turbulent velocity standard deviation (open squares) in the Tombstone canopy with model prediction obtained by equilibrium partitioning of the turbulence kinetic energy.....	30
Figure 5. Comparison of the observed profile of vertical turbulent velocity standard deviation (open squares) in the Tombstone canopy with model prediction by equilibrium partitioning of the turbulence kinetic energy.....	31
Figure 6. Comparison of the observed profile of the streamwise turbulent velocity standard deviation (open squares) in the Tombstone canopy with model prediction obtained by algebraic stress model partitioning of the turbulence kinetic energy.....	32
Figure 7. Comparison of the observed profile of the vertical turbulent velocity standard deviation (open squares) in the Tombstone canopy with model prediction obtained by algebraic stress model partitioning of the turbulence kinetic energy.....	33
Figure 8. Comparison of the observed values of the attenuation coefficient at various plan area indices for staggered and square arrays of cubical obstacles with two proposed parameterizations.....	34
Figure 9. The observed variation of the skin friction at canopy height as a function of the plan area index for staggered and square arrays of cubical obstacles.....	35
Figure 10. Model predictions of profiles of the turbulence kinetic energy for a square array of cubical obstacles with various plan area indices.....	36
Figure 11. Model predictions of profiles of streamwise turbulent velocity standard deviation for a square array of cubical obstacles with various plan area indices. The modeled profiles were obtained using equilibrium partitioning of the turbulence kinetic energy. The horizontal bars show the range in the observations by Macdonald et al. [21].....	37

Figure 12. Model predictions of profiles of vertical turbulent velocity standard deviation for a square array of cubical obstacles with various plan area indices. The modeled profiles were obtained using equilibrium partitioning of the turbulence kinetic energy.	38
Figure 13. Model predictions of profiles of streamwise turbulent velocity standard deviation for a square array of cubical obstacles with various plan area indices. The modeled profiles were obtained using algebraic stress model partitioning of the turbulence kinetic energy. The horizontal bars show the range in the observations by Macdonald et al. [21].	39
Figure 14. Model predictions of profiles of vertical turbulent velocity standard deviation for a square array of cubical obstacles with various plan area indices. The modeled profiles were obtained using algebraic stress model partitioning of the turbulence kinetic energy.	40
Figure 15. Model predictions of profiles of streamwise turbulent velocity standard deviation for a square array of cubical obstacles at high plan area indices. The modeled profiles were obtained using equilibrium partitioning of the turbulence kinetic energy. Open symbols are measurements made by Macdonald et al. [21].	41
Figure 16. Model predictions of profiles of streamwise turbulent velocity standard deviation for a square array of cubical obstacles at high plan area indices. The modeled profiles were obtained using algebraic stress model partitioning of the turbulence kinetic energy. Open symbols are measurements made by Macdonald et al. [21].	42

Introduction

Incidents in Tokyo involving the use of chemical and biological warfare (CBW) agents by a terrorist organization have mobilized both military and public concerns on the use of these weapons against military and civilian populations in built-up or urban areas consisting of large groups of obstacles. In response to these increasing concerns, the prediction of the dispersion of CBW agents released within an urban area has recently become the subject for many investigations since information obtained from urban dispersion models will be used to form the basis on which government and military commanders (as well as other decision makers) will respond and act to mitigate the effects of a particular incident. Physically-based models such as Lagrangian Stochastic (LS) models exist for the prediction of plume or cloud dispersion in complex environments, and certainly can be applied to the problem of urban dispersion. The prediction of dispersion using LS models, which involves the calculation of the trajectories of a large number of tagged fluid particles representing the contaminant mass and the derivation of the ensemble-average concentration from the calculated particle distribution, is enticingly simple in concept and general in approach. However, for urban dispersion, LS models require to be provided information on the mean and statistical properties of the turbulent wind field within and above the urban canopy (e.g., mean wind speed, shear stress, velocity variances, etc.).

The mean flow and turbulence within and immediately above an urban canopy (wherein the atmospheric flow is influenced by the individual roughness elements or obstacles) possess a fully three-dimensional structure. Although the development of three-dimensional dynamical models of the mean flow and turbulence in simplified urban canopies consisting of large groups of regularly spaced obstacles is progressing, these models tend to require extensive computational resources. These flow models involve the solution of the conservation equations of mass, momentum, and energy, and the detailed information obtained from these models can be used to "drive" physically-based dispersion models to provide estimates of the contaminant concentrations. However, currently the computational demands of these three-dimensional models will preclude their use for emergency response situations which require the ability to generate a dispersion prediction in a time frame that will permit protective actions to be taken. In view of this, we argue that for many practical applications it is convenient to consider spatial averages of the mean wind and turbulence within an urban canopy obtained by averaging horizontally the mean wind and turbulence statistics over an area that is much greater than the spacings between the individual roughness elements comprising the urban canopy. This provides a simplified one-dimensional mean wind and turbulence model for urban canopy flow whereby the flow statistics depend only on the

height z . In this simplified description of urban flow, the spatially-averaged mean wind and turbulence vary only with height, and the detailed three-dimensional description of flow and turbulence characteristics about the individual buildings is lost.

The primary objective of this report is to describe and test a simple, analytical one-dimensional model for the prediction of mean flow and turbulence within and above an urban canopy. This model was developed originally for vegetative canopies (e.g., forests, cereal crops, etc.), but will be applied here to urban canopies. While there are similarities between vegetative and urban canopies, there are enough important differences between these two types of canopies (e.g., characteristic density of roughness elements and their stiffness or ability to react to the drag forces) to require an independent evaluation of the model for the urban canopy application. It is hoped that this simple, analytical one-dimensional model for urban canopy flows can be used to provide useful input information on the statistics of the wind field required to drive LS models of urban dispersion.

Model for mean velocity field and shear stress

If the terrain is reasonably homogeneous at the mesoscale, Monin-Obukhov similarity theory provides a simple and practical method for the description of the mean wind profile and shear stress above the roughness sublayer, where the perturbations on the wind arising from the roughness elements have decayed. In this section, we are concerned with the specification of simple, one-dimensional models for the spatially-averaged mean wind and shear stress within the urban canopy (viz., within the roughness elements comprising the urban canopy). Unless otherwise indicated, all flow variables of interest in what follows refer to the bulk or spatially-averaged characteristics of the flow obtained by averaging over a thin, horizontal slab with a characteristic length scale that is much greater than the characteristic spacings between the individual obstacles. The urban canopy is assumed to be horizontally uniform, so that after the spatial averaging the mean flow and turbulence within the canopy show a systematic variation in the vertical direction only.

To begin, a particular *ansatz* is chosen to model the mean wind speed $U(z)$ within the canopy; namely,

$$U(z) = U(h_c) \exp(-\alpha(1 - z/h_c)), \quad (1)$$

where α is the attenuation coefficient and h_c is the height of the canopy. This is the exponential profile that was first suggested by Inoue [1] and Cionco [2] as an appropriate wind profile within vegetative canopies. Cionco [3] has obtained values of α for different vegetative canopies by fitting the *ansatz* of Equation (1) to measured velocity profiles. He indicated that α lies in the range between 1 and 3 for moderately dense arrays of semi-rigid roughness elements (such as mature corn and some types of trees). It should be noted that it is possible to “derive” the empirical exponential wind profile by starting with the mean streamwise momentum balance equation [cf. Equation (2) below], using a flux gradient model for the shear stress $[\overline{u'w'} = -K_m dU/dz]$, where K_m is a turbulent transport coefficient (eddy viscosity), and using the Prandtl-von Kármán mixing length theory to specify the eddy viscosity as $K_m = l^2 dU/dz$, where the mixing length l is most simply taken as a constant within the canopy.

Assuming that the flow is stationary with no mean streamwise pressure gradient, the mean momentum equation for the spatially-averaged mean wind U within a canopy reduces to a balance between the vertical divergence of the kinematic shear stress $\tau(z) \equiv -\overline{u'w'}(z)$ and the form or pressure drag, so

$$\frac{d\tau}{dz} = C_d A U^2(z), \quad (2)$$

where C_d is the obstacle *in situ* drag coefficient that accounts for the effects of the drag of canopy turbulence and also for the sheltering within the canopy, and A is the frontal area density which is defined as the frontal area of the individual obstacles per unit volume of the canopy. In view of Equations (1) and (2), it follows that the shear stress must have the following form since its z -derivative is proportional to the square of the mean wind speed:

$$-\overline{u'w'}(z) = u_*^2 \exp(-2\alpha(1 - z/h_c)), \quad (3)$$

where $u_* \equiv (-\overline{u'w'}(z \geq h_c))^{1/2}$ is the friction velocity above the canopy. It is assumed implicitly that a constant stress layer exists above the canopy. If we substitute Equation (3) into Equation (2), it is found that the attenuation coefficient has the explicit form

$$\alpha = \frac{C_d A h_c}{2u_*^2/U^2(h_c)}. \quad (4)$$

It is worth noting that α is the ratio of the non-dimensional drag parameter $C_d A h_c$ (which embodies information about the bulk canopy structure) and the skin friction $2u_*^2/U^2(h_c)$ (which contains information about the interaction of the airflow with the canopy at canopy height and, as such, can be interpreted as a bulk drag coefficient).

Massman [4] showed how the model for the mean wind U and shear stress τ can be generalized to accomodate an arbitrary canopy structure, viz., a canopy where C_d and/or A can be functions of z). The modification of the mean wind and shear stress profiles in this case is minor—it merely involves substituting for z/h_c in Equations (1) and (3), the variable $\zeta(z)/\zeta(h_c)$. Here, $\zeta(z)$ is taken as the new independent variable that is defined in terms of height z above the ground surface beneath the canopy elements as

$$\zeta(z) = \int_0^z C_d(z') A(z') dz'. \quad (5)$$

Furthermore, in the case of a canopy of arbitrary structure, the attenuation coefficient in Equation (4) has $\zeta(h_c)$ substituted for the non-dimensional drag parameter $C_d A h_c$ in the numerator. However, because such detailed information on $C_d(z)$ and/or $A(z)$ is usually unavailable, we prefer to represent the bulk canopy structure using a constant effective or bulk drag parameter $(C_d A)_b$, which for the case of a canopy with arbitrary structure $C_d(z)$ and $A(z)$ would simply be defined as [cf. Equation (2)]

$$\tau(h_c)/u_*^2 = 1 = (C_d A)_b \int_0^1 \left(\frac{U}{u_*}\right)^2 d\frac{z}{h_c} \equiv \int_0^1 C_d(z) A(z) \left(\frac{U}{u_*}\right)^2 d\frac{z}{h_c}. \quad (6)$$

In fact, in all cases $C_d(z)A(z)$ is simply treated as an adjustable model function (rather than as a strict model input) that is obtained by tuning the function to match either the

model prediction of the mean wind against available observations, or by diagnosing the function from the observed shear stress divergence. Currently, there does not exist a theory that could be used to predict the drag parameter from a knowledge of the canopy topology and the aerodynamic drag of the roughness elements (obstacles) in isolation. In view of these uncertainties, there does not seem to be much gained in trying to use a local drag parameter $C_d(z)A(z)$ in the flow specification in place of the simpler constant effective drag parameter $C_d A$.

The specification of the mean wind profile of Equation (1) or the shear stress profile of Equation (3) can be used to determine the displacement height d for the canopy. Thom [5] first observed, and Jackson [6] subsequently demonstrated theoretically that d can be interpreted as the mean height of momentum absorption by the canopy, which in view of Equation (2) can be also interpreted as the level at which the mean drag force in the canopy appears to act. Hence,

$$\begin{aligned}\frac{d}{h_c} &= 1 - \int_0^1 \frac{-\overline{u'w'}}{u_*^2} d\frac{z}{h_c} \\ &= \int_0^{h_c} zU^2(z) dz / \int_0^{h_c} U^2(z) dz.\end{aligned}\quad (7)$$

Insertion of either Equation (3) into the first part of Equation (7) or, equivalently, insertion of Equation (1) into the second part of Equation (7) leads to the following explicit expression for the displacement length:

$$d/h_c = 1 - \frac{1}{2\alpha} (1 - \exp(-2\alpha)). \quad (8)$$

Finally, the model here can be used to provide an estimate for the roughness length of the canopy in terms of the attenuation coefficient α and the drag parameter $C_d A$. If we assume that the semi-logarithmic mean wind profile in the inertial sublayer can be extrapolated down to the top of the canopy at $z = h_c$, we have

$$z_0/h_c = (1 - d/h_c) \exp\left(-\kappa \frac{U(h_c)}{u_*}\right), \quad (9)$$

where κ is von Kármán's constant. Now, if we substitute for d/h_c from Equation (8) and $U(h_c)/u_*$ from Equation (4), we get

$$z_0/h_c = \frac{1}{2\alpha} (1 - \exp(-2\alpha)) \exp\left(-\kappa (2\alpha/C_d A h_c)^{1/2}\right). \quad (10)$$

This page intentionally left blank

Model for the TKE and velocity variances

The key to the determination of the velocity variances centers on the construction of an analytical solution to a simplified transport equation for the turbulence kinetic energy (TKE) k . Massman and Weil [7] showed how to construct a simple analytical model for k based on the second-order closure model for canopy flows developed by Wilson and Shaw [8]. The transport equation for $k \equiv (\sigma_u^2 + \sigma_v^2 + \sigma_w^2)/2$ (where σ_u , σ_v , and σ_w are the streamwise (x), cross-stream (y), and vertical (z) components of the velocity standard deviations, respectively) implied by the second-order closure model for turbulence statistics of Wilson and Shaw [8] assumes the following form:

$$\frac{d}{dz} \left(\sigma_e \lambda_1 \frac{d\sigma_e^2}{dz} \right) - \frac{14\sigma_e^3}{9\lambda_3} + \frac{2\sigma_e}{9\lambda_2} (\sigma_w^2 - \sigma_e^2/3) + 2C_d A U^3 + 2(-\overline{u'w'}) \frac{dU}{dz} = 0, \quad (10)$$

where σ_e^2 is twice the turbulence kinetic energy (i.e., $k \equiv \sigma_e^2/2$). From left to right, the terms in the transport equation for σ_e^2 represent the following physical processes: (1) turbulent transport of σ_e^2 ; (2) rate of viscous dissipation of σ_e^2 , which converts turbulence kinetic energy to heat; (3) return-to-isotropy, expressing the rate at which turbulence energy is redistributed between the three components of the velocity variance; (4) wake production, accounting for the production of turbulence kinetic energy from the mean kinetic energy of the flow in the wakes of the roughness elements (obstacles); and, (5) shear production, accounting for the conversion of the mean kinetic energy to turbulence kinetic energy due to the action of the shear stress against the mean velocity shear. It should be emphasized that the return-to-isotropy term does not normally appear in the transport equation for the turbulence kinetic energy, but its presence in this case results from the particular closure assumptions adopted by Wilson and Shaw [7] for their second-order closure model for canopy flow.

To close Equation (10), it is necessary to parameterize the three canopy length scales λ_i ($i = 1, 2, 3$). Wilson and Shaw [7] made the assumption that these three length scales vary with height z within the canopy in a similar fashion, so $\lambda_i(z) = \nu_i l(z)$, where ν_i ($i = 1, 2, 3$) are constants and l is a characteristic length scale. Generally, the parameterization scheme used by Wilson and Shaw prescribed the characteristic length scale $l(z)$ as a function of the density and drag properties of the (vegetative) canopy and height above the surface such that the length l is continuous and assumes the maximum possible value allowed by the following constraints: (1) $l = 0$ at $z = 0$; (2) $l \leq \alpha_*/(C_d A)$ for $0 < z < h_c$; and, (3) $|dl/dz| \leq \kappa$ for $z > 0$, where α_* is a constant, with α_* and C_d chosen to obtain the best fit to observed canopy flow data. However, to ensure that an analytical solution can be constructed for

Equation (10), Massman and Weil [7] relaxed some of these constraints and simply assumed that the characteristic length scale can be parameterized as $l(z) = \alpha_*/(C_d(z)A(z))$. Note that for the case we are interested in, $l(z)$ is a constant throughout the canopy since $C_d A$ is assumed to be a constant. The constants ν_i in the definition of λ_i are chosen to be consistent with the constant stress layer and semi-logarithmic mean wind profile that is assumed to exist immediately above the canopy. In particular, it is assumed that immediately above the canopy, the velocity standard deviations σ_i are constant and proportional to the friction velocity (i.e., $\sigma_i = \gamma_i u_*$, where γ_i ($i = 1, 2, 3$) are constants that are assumed to be known from the properties of the constant stress layer above the canopy). To be consistent with the specified properties of the constant stress layer, the closure coefficients ν_i must be chosen as follows: $\nu_1 = (\gamma_1^2 + \gamma_2^2 + \gamma_3^2)^{-1/2}$, $\nu_3 = (\gamma_1^2 + \gamma_2^2 + \gamma_3^2)^{3/2}$, and $\nu_2 = \nu_3/6 - \gamma_3^2/(2\nu_1)$. With these relationships for the closure coefficients ν_i and the parameterization for the characteristic length scale l , the transport equation for σ_e in Equation (10) reduces to (assuming a constant drag parameter $C_d A$)

$$\frac{d^2 \sigma_e^3}{dz^2} = \Lambda^2 (C_d A)^2 \sigma_e^3 - \frac{3}{\alpha_* \nu_1} (C_d A)^2 U^3 - \frac{3}{\alpha_* \nu_1} (C_d A) (-\overline{u'w'}) \frac{dU}{dz}, \quad (11)$$

where $\Lambda^2 \equiv 3\nu_1^2/\alpha_*^2$. Massman and Weil [7] showed that Equation (11) possesses the following analytical solution subject to the upper boundary condition at $z = h_c$ specified by $\sigma_e^3(z = h_c)/u_*^3 = \nu_3$:

$$\begin{aligned} \frac{k^{1/2}}{u_*} &\equiv \frac{1}{\sqrt{2}} \frac{\sigma_e}{u_*} \\ &= \frac{1}{\sqrt{2}} \left[\nu_3 e^{-\Lambda C_d A h_c (1-z/h_c)} + B_1 \left(e^{-3\alpha(1-z/h_c)} - e^{-\Lambda C_d A h_c (1-z/h_c)} \right) \right]^{1/3}, \quad (12) \end{aligned}$$

where $B_1 \equiv -(9u_*/U(h_c))/(2\alpha_* \nu_1 [9/4 - \Lambda^2 u_*^4/U^4(h_c)])$.

The expression for the turbulence kinetic energy k in Equation (12) can be used to obtain predictions for the velocity variances. The simplest method is simply to derive the velocity variances from the calculated turbulence kinetic energy by assuming equilibrium partitioning. In this approach, it is assumed that the component velocity variances in the canopy are proportional to the turbulence kinetic energy and that the proportionality constants are the same as those in the constant stress layer overlying the canopy. In consequence, equilibrium partitioning provides the following predictions for the standard deviations of the velocity within the canopy:

$$\sigma_i(z) = \frac{\gamma_i}{(\gamma_1^2 + \gamma_2^2 + \gamma_3^2)^{1/2}} (2k(z))^{1/2}, \quad z \leq h_c, \quad (13)$$

where k is determined by Equation (12). Note that using equilibrium partitioning, the turbulent velocity variances are scaled versions of the turbulence kinetic energy and, hence, have exactly the same shape.

An alternative to equilibrium partitioning for the derivation of the velocity variances would be to apply an algebraic stress model (ASM). The algebraic stress model that is used here is derived from the well understood and successful second-order closure model developed by Launder, Reece, and Rodi [9] with the incorporation of additional terms to describe the physics particular to canopy flows. For three-dimensional canopy flows, it can be shown after some rather lengthy and tedious algebraic manipulations (Yee, 1999, unpublished) that this ASM leads to the following form for the anisotropy tensor $a_{ij} \equiv \overline{u'_i u'_j} / k - \frac{2}{3} \delta_{ij}$, (δ_{ij} is the Kronecker delta function):

$$\frac{a_{ij}}{g^*} + b_2 \left(S_{ik} a_{kj} + S_{jk} a_{ki} - \frac{2}{3} S_{lk} a_{kl} \delta_{ij} \right) + b_3 (W_{ik} a_{kj} + W_{jk} a_{ki}) = -b_1 S_{ij}, \quad (14)$$

where

$$S_{ij} \equiv \frac{1}{2} \frac{k}{\epsilon} \left(\frac{\partial U_i}{\partial x_j} + \frac{\partial U_j}{\partial x_i} \right) \quad (15)$$

is the normalized mean rate-of-strain tensor (viz., normalized by the turbulence time scale k/ϵ , where ϵ is the viscous dissipation rate);

$$W_{ij} \equiv \frac{1}{2} \frac{k}{\epsilon} \left(\frac{\partial U_i}{\partial x_j} - \frac{\partial U_j}{\partial x_i} \right) \quad (16)$$

is the normalized mean vorticity (rotation) tensor;

$$g^* \equiv \frac{1}{c_1 + P_s/\epsilon + P_w/\epsilon - 1}; \quad (17)$$

and,

$$b_1 \equiv \frac{8}{15}, \quad b_2 \equiv \frac{5 - 9c_2}{11}, \quad b_3 \equiv \frac{7c_2 + 1}{11}, \quad (18)$$

are numerical constants. Furthermore, c_1 and c_2 are closure constants that arise in the Launder, Reece, and Rodi [9] parameterization of the pressure-strain term. Note that g^* [cf. Equation (17)] embodies the information on the net production (shear P_s and wake P_w) per unit dissipation of the TKE. Equation (14) constitutes a closed system of algebraic equations for the determination of the Reynolds stress anisotropy in terms of the mean velocity gradients. Once the mean flow and TKE and its dissipation are known, Equation (14) can then be solved numerically at each point in the flow domain for the anisotropy stress components (whose normal stress components along the diagonal, in turn, determines the partitioning of the TKE).

Equation (14) simplifies considerably for the spatially-averaged flow variables (mean wind and turbulence statistics) describing an effectively horizontally homogeneous canopy. For flow variables that depend only on z , Equations (14) to (18) reduce to the following form:

$$\frac{a_{11}}{g^*} = \frac{8 + 12c_2}{33} \times (-2S_0 a_{13}); \quad (19)$$

$$\frac{a_{22}}{g^*} = \frac{18c_2 - 10}{33} \times (-2S_0 a_{13}); \quad (20)$$

$$\frac{a_{33}}{g^*} = \frac{2 - 30c_2}{33} \times (-2S_0 a_{13}). \quad (21)$$

Here, $a_{11} \equiv \sigma_u^2/k - 2/3$, $a_{22} \equiv \sigma_v^2/k - 2/3$, and $a_{33} \equiv \sigma_w^2/k - 2/3$. Also, $S_0 \equiv \frac{1}{2} \frac{k}{\epsilon} dU/dz$ is the normalized mean rate-of-strain, $a_{13} \equiv \overline{u'w'}/k$ is the normalized kinematic shear stress, and g^* is given by Equation (17) with $P_s = -\overline{u'w'}dU/dz$ (shear production) and $P_w = \frac{1}{2}C_d AU^3$ (wake production, or work done by the mean flow against form drag). To complete the ASM partitioning of the velocity variances, we need a model for the TKE dissipation rate $\epsilon(z)$. Although Massman and Weil [7] provide a model for $\epsilon(z)$, we prefer to use a TKE dissipation rate model suggested by Wilson, Finnigan, and Raupach [10] that explicitly distinguishes between shear-generated and wake-generated turbulence. Here, the TKE dissipation, ϵ , is modelled as $\epsilon = \max(\epsilon_{cc}, \epsilon_{fd})$ where:

$$\epsilon_{cc} = \frac{(c_e k)^{3/2}}{\lambda}, \quad \epsilon_{fd} = \beta_* C_d A U k. \quad (22)$$

The term ϵ_{cc} is the standard parameterization for free-air viscous dissipation, the only TKE sink above the canopy. The specification for ϵ_{fd} ('form drag'), which converts resolved TKE to the small, rapidly dissipated 'wake-scales', can be justified on physical grounds. The constant $c_e = u_*^2/k(z = h_c)$ is the shear stress to TKE ratio at the canopy top ($z = h_c$). The closure coefficient $\beta_* = 1$ was suggested by Wilson, Finnigan, and Raupach [10]. The turbulence length scale λ is determined from $\lambda = \max(\lambda_i, \lambda_o)$, where

$$\frac{1}{\lambda_i} = \frac{1}{\kappa z} + \frac{1}{\lambda_c}, \quad \frac{1}{\lambda_o} = \frac{1}{\kappa(z-d)} + \frac{1}{L_\infty}, \quad (23)$$

where

$$\lambda_c = (k(z = h_c))^{1/2} / dU/dz|_{z=h_c} \quad (24)$$

is a canopy shear length scale measuring the strength of the wind shear at the canopy top that Raupach, Finnigan, and Brunet [11] have identified as being a critical length scale governing the eddy transport within a canopy. Here, λ_i is an 'inner' scale, λ_o is an 'outer' scale, and L_∞ is an imposed limiting length scale that restricts the depth of the inertial sublayer overlying the canopy.

The closure coefficients c_1 and c_2 arising, respectively, from the return-to-isotropy and rapid part of the Launder, Reece, and Rodi [9] parameterization of the pressure-strain redistribution term in the transport equation for the Reynolds stress tensor, can be set by the physical properties of the flow in the logarithmic constant stress layer assumed to overlie the canopy. Again, if in this constant stress layer, $\sigma_i = \gamma_i u_*$ ($i = 1, 2, 3 \equiv u, v, w$), then it

follows that (assuming in this layer that the production of TKE is equal to its dissipation, corresponding to the condition of local equilibrium)

$$\left(\gamma_u^2 c_e - \frac{2}{3}\right) c_1 - \frac{4}{11} c_2 = \frac{8}{11}, \quad (25)$$

$$\left(\gamma_v^2 c_e - \frac{2}{3}\right) c_1 - \frac{6}{11} c_2 = -\frac{10}{33}, \quad (26)$$

$$\left(\gamma_w^2 c_e - \frac{2}{3}\right) c_1 + \frac{10}{11} c_2 = -\frac{2}{33}. \quad (27)$$

Here, $c_e^{-1} \equiv \frac{1}{2}(\gamma_u^2 + \gamma_v^2 + \gamma_w^2)$ is the prescribed (observed) equilibrium value at canopy top of the ratio of the TKE to the shear stress [cf. Equation (22)]. Given the relations in Equations (25) to (27), specified values for γ_u , γ_v , and γ_w will yield values for c_1 , c_2 , and c_e . Typically, for most turbulent boundary layers, $\gamma_u \approx 2.4$, $\gamma_v \approx 1.9$, and $\gamma_w \approx 1.25$ implying that $c_e \approx 0.18$. For a wide range of thin shear flows in equilibrium, the shear stress/TKE ratio (i.e., the constant c_e) is relatively constant. Indeed, various measurements which have been summarized by Townsend [12] indicate that for boundary layers, wakes, and mixing layers, the ratio is nearly the same and varies between about 0.2 to 0.3. The constant c_e in the engineering literature is often referred to as Bradshaw's constant, and sometimes as Townsend's constant (although the latter is defined in our current notation to be $c_e/2$).

This page intentionally left blank

Parameterizations for model inputs

The key inputs to the model are the “skin friction”, $u_*^2/U^2(h_c)$, (actually, the skin friction c_f is twice this value) and either the attenuation coefficient, α , or the normalized drag parameter, $C_d Ah_c$ [cf. Equation (4)] Furthermore, we need to know the equilibrium values of k/u_*^2 (which we have defined to be c_e^{-1}), and σ_i/u_* ($i = 1, 2, 3 \equiv u, v, w$) at the canopy top. Only two of the values σ_i/u_* need to be known at the canopy top in addition to k/u_*^2 since $k/u_*^2 = \frac{1}{2}(\sigma_u^2/u_*^2 + \sigma_v^2/u_*^2 + \sigma_w^2/u_*^2)$. However, the critical input values are $u_*^2/U^2(h_c)$ and $C_d Ah_c$ (or, α), since the values of σ_i/u_* ($i = 1, 2, 3$) and/or c_e does not appear to vary greatly from canopy to canopy, or from one local equilibrium layer to another.

If observed values for $u_*^2/U^2(h_c)$ and $C_d Ah_c$ (or, α) are available for a particular canopy, then they can be used directly in the model. For general applications of the model, when observed values for $u_*^2/U^2(h_c)$ and α are not available, parameterizations for these quantities are required. For vegetative canopies, Massman [4] suggested the following parameterization for the skin friction at canopy top:

$$u_*/U(h_c) = k_1 - k_2 \exp(-k_3 C_d Ah_c), \quad (28)$$

where $k_1 = 0.320$, $k_2 = 0.264$, and $k_3 = 15.1$ are model constants. Also, Raupach [13, 14] developed for random arrangements of obstacles that are not too densely spaced together, a parameterization for the skin friction that is expressed as an implicit function of the frontal area index λ_F (i.e., ratio of the frontal area of the elements facing the wind to the total ground area occupied by the elements):

$$U(h_c)/u_* = \frac{\exp(c\lambda_F U(h_c)/(2u_*))}{(C_s + \frac{1}{2}C_d \lambda_F)^{1/2}}, \quad (29)$$

where C_s is the drag coefficient of the substrate, C_d is the drag coefficient of the obstacles in isolation, and $c \approx 0.5$ is an empirical shelter coefficient that is determined by the rate at which a roughness element wake spreads in the cross-stream direction. Because Raupach's model cannot properly describe overlapping of sheltering in densely packed roughness arrays, it can only be used for λ_F less than about 0.1 to 0.2.

For regularly spaced arrays of bluff roughness elements (urban canopies), much of the effort has focussed on the parameterization of the roughness length, z_0 , as a function of the frontal area index, λ_F . However, these parameterizations for z_0 must imply implicitly also a parameterization for the skin friction. In particular, all these parameterizations start

with the assumption that the semi-logarithmic velocity profile in the inertial sublayer (lying above the canopy) can be extrapolated down to the canopy top at $z = h_c$ such that the skin friction $u_*^2/U^2(h_c)$ is linked to z_0 as

$$\frac{z_0}{h_c} = \left(1 - \frac{d}{h_c}\right) \exp\left(-\kappa \frac{U(h_c)}{u_*}\right). \quad (30)$$

The error in this assumption is small, and is discussed in detail in Hanna and Britter [15]. Many parameterizations for z_0 involve modeling $U(h_c)/u_*$ as a function of the topological parameters that characterize the urban canopy. For example, the Macdonald et al. [16] parameterization for z_0 for regular arrays of obstacles (square and staggered) effectively uses the following expression for the skin friction in Equation (30):

$$\frac{u_*^2}{U^2(h_c)} = \frac{1}{2} \beta C_d \left(1 - \frac{d}{h_c}\right) \lambda_F, \quad (31)$$

where C_d is the drag coefficient of an isolated roughness element mounted on the surface and β is a correction factor (empirical parameter) for the drag coefficient that includes the influences of the incident turbulence length scale, the incident wind angle, the presence of rounded corners in the obstacles, and the geometry of the roughness array. For square and staggered arrays of cubical obstacles, Macdonald et al. [17] calibrated this relationship using their wind tunnel data and recommended values of 0.55 and 1.0 for β , for square and staggered arrays of cubical obstacles, respectively. An alternative parameterization has been suggested by Duijm [16] who uses

$$\frac{u_*^2}{U^2(h_c)} = \frac{1}{2} C_d \lambda_{F,eff}, \quad (32)$$

in the parameterization for z_0/h_c in Equation (30). Here, $\lambda_{F,eff}$ is an effective frontal area index that accounts for the sheltering and assumes the form

$$\lambda_{F,eff} = \lambda_F \left(1 - S \frac{d_{pl}}{h_c}\right), \quad (33)$$

where S is an empirical sheltering efficiency factor of order one and d_{pl} is an in-plane displacement height that was originally introduced by Bottema [18, 19] to account for the effect of sheltering and the presence of recirculation zones.

It is not possible based on the available data to recommend a particular parameterization for z_0 . The large uncertainties in the determination of z_0 (especially from mean velocity profiles above the canopy) and the large scatter in the measurements of z_0 (cf. Grimmond and Oke [20]) do not provide a standard that can be used to distinguish between the

different parameterizations for z_0 proposed in the literature. Indeed, Bottema [18] and Grimmond and Oke [20] provide a comprehensive survey of data on z_0 obtained from various urban canopies, and strongly emphasize that there are numerous reasons for doubting their correctness. In consequence, the various parameterizations for z_0 represent nothing more than ad-hoc formulae that can only really be justified by their success in fitting the limited observations used for their development.

The remaining parameter that needs to be specified is the attenuation coefficient α . Best values of α for numerous canopies (but, primarily vegetative) have been compiled by Cionco [3]. More recently, Macdonald et al. [21] found least-squares fitted values for α for regular roughness arrays (urban canopies) of cubical obstacles with plan area indices (i.e., ratio of obstacle plan area to total ground area occupied by the obstacles) in the range from about 0.05 to 0.30. These researchers used this data to recommend the following relationship between α and the plan area index λ_p for $\lambda_p \in (0.05, 0.30)$:

$$\alpha = -0.24 + 12.5\lambda_p. \quad (34)$$

This page intentionally left blank

Results

Massman and Weil [7] tested the one-dimensional analytical model for canopy flow against a number of horizontally homogeneous vegetative canopies, primarily to determine an appropriate value for the closure coefficient α_* required to define the characteristic length scale $l(z)$. To this purpose, these researchers calibrated the model against corn canopy data from Shaw et al. [22] and Wilson et al. [23], spruce and aspen forest data from Amiro [24], Douglas fir forest canopy data from Lee and Black [25], pine forest data from Katul and Albertson [26], and a wind tunnel 'wheat' canopy data from Brunet et al. [27]. This calibration procedure involved some rather fine-tuning to the data consisting of adjusting the variable drag coefficient $C_d(z)$ to provide the best fits of the model predictions to the observed canopy profiles of mean wind $U(z)$ and shear stress $-\overline{u'w'}(z)$, and then adjusting the parameter α_* to provide an optimal fit to the observed canopy profiles of the turbulent velocity standard deviations σ_u and σ_w . Based on this trial and error adjustment to the observed data, Massman and Weil [7] found that the values for α_* were generally between about 0.04 and 0.06. Using these results, they recommended that a value of $\alpha_* = 0.05$ be used for general model application.

In this section, we make model comparisons with data from "urban" canopies (i.e., roughness element arrays composed of solid bluff obstacles, rather than flexible elements that are characteristic of vegetative canopies). Unfortunately, there is a dearth of data on observed profiles of mean wind speed and turbulence statistics within an urban canopy. The first urban canopy considered is described in detail by Raupach, Coppin, and Legg [28]. This canopy (referred to as the Tombstone canopy) consisted of an extensive array of thin, "billboard-shaped" obstacles (or, vertical bars) with dimensions 60 mm high, 10 mm wide, and 1 mm thick, arranged in a staggered pattern with a spacing of 60 mm in the cross-stream direction and 44 mm in the streamwise direction to give a frontal area index for the array of 0.23. For specific comparisons between the model predictions and the observations, the drag parameter $C_d Ah_c$, skin friction $u_* / U(h_c)$, and the γ_i 's (i.e., ratio of the velocity standard deviation in the i -th direction to the friction velocity at the canopy top) were taken from the observations.

Figures 1 and 2 compare measured profiles of the mean wind speed and kinematic shear stress for the Tombstone canopy with the model predictions. It is seen that the attenuation coefficient, α , inferred from the observed values of the drag parameter and skin friction factor [cf. Equation (4)] is too large, causing the predicted mean wind speed and shear stress to decay too rapidly within the canopy. Least-squares fitting of the exponential profile

(cf. Equation (1)) to the observed profile of $U(z)$ gave a value of 1.41 for α , rather than the larger inferred value of 1.78. Using this fitted value for α gave reasonable predictions for the mean wind speed and shear stress within the Tombstone canopy. In consequence, for the comparisons of model predictions with observations for the turbulence kinetic energy and turbulent velocity standard deviations, we will use $\alpha = 1.41$ in the analytical model unless otherwise indicated.

Figure 3 shows a comparison of the observed and modeled turbulence kinetic energy for the Tombstone canopy. Using the value of $\alpha_* = 0.05$ recommended by Massman and Weil [7], it is seen that the model predictions for k with attenuation coefficients of 1.78 (inferred value) and 1.41 (least-squares fitted value) provide, respectively, a lower and upper bound for the observed values of k . However, the model profile for k with $\alpha_* = 0.055$ (chosen by trial and error) and the least-squares fitted value of $\alpha = 1.41$ seems to provide the best visual comparison with the observed k profile. However, even so, this model profile underestimates k in the region at about mid-canopy height.

Figures 4 and 5 show the measured and modeled profiles for σ_u and σ_w , respectively. The modeled profiles for the normal stresses here were obtained using equilibrium partitioning of the turbulence kinetic energy. It is seen that agreement between observation and model predictions for σ_u for the case with $\alpha = 1.41$ and $\alpha_* = 0.055$ is good. However, the model profile for σ_w for this case does not agree as well with the observed profile, primarily because the observed profile for σ_w shows more concavity than that for σ_u . In particular, the model profile for σ_w with $\alpha = 1.41$ and $\alpha_* = 0.055$ underestimates the observed values in the upper part of the canopy. Because the model profiles for the turbulent velocity standard deviations obtained by equilibrium partitioning are essentially constructed by applying scaling factors to the associated model profile for k , all these profiles have necessarily the same shape. Hence, because of the differences in shape of the observed profiles for σ_u and σ_w , it is not possible for the equilibrium partitioning of k to provide model profiles for the turbulent velocity standard deviations that can fit both the observed profiles for σ_u and σ_w .

Figures 6 and 7 display the measured and modeled profiles for σ_u and σ_w , respectively. The modeled profiles here are obtained by the algebraic stress partitioning of the TKE. The agreement of the model and observations is excellent for σ_u with $\alpha = 1.41$ and $\alpha_* = 0.055$, but the corresponding model profile for σ_w underestimates the measurements for the vertical velocity standard deviation in the middle to upper part of the canopy. In spite of the fact that algebraic stress partitioning of the TKE can produce different shapes for the component velocity variance profiles, the agreement obtained for σ_w was no better than that procured from the equilibrium partitioning (at least for the Tombstone canopy).

Macdonald et al. [21] made measurements of the mean wind speed and streamwise turbulent velocity standard deviation in urban canopies comprised of arrays of regularly spaced cubical obstacles with plan area indices ranging from about 0.05 to 0.9. These researchers demonstrated that for plan area indices less than about 0.2, the measured mean wind speed within the canopy is well modeled using the exponential wind profile of Equation (1). Although the plan area index λ_p is used to denote a proportion, the most convenient symbolism for theoretical interpretation, most users of this quantity prefer to do their arithmetic in terms of percentages, and in calculations the same symbols will be used even though $100\lambda_p$ would be more correct. No confusion should be caused by this slight ambiguity of symbolism. Figure 8 displays the variation of the attenuation coefficient α as a function of the plan area index λ_p for both square and staggered arrays, indicating that there are only minor differences between the two array geometries. Macdonald et al. [21] recommended the following relationship between α and λ_p : $\alpha = -0.24 + 0.125\lambda_p$ (with λ_p expressed as a percentage). However, this relationship predicts that $\alpha < 0$ for $\lambda_p \lesssim 2$ percent. To remove this physical inconsistency, we re-fitted the data using a power-law relationship of the form $\alpha = A\lambda_p^s$ where s is the power-law exponent. The best power-law fit to the data is shown in Figure 8 and yielded the following result: $\alpha = 0.104\lambda_p$ (with λ_p expressed as a percentage). Note that in this power-law fit, $s = 1$ almost exactly.

The observed values of the skin friction factor at canopy top for the staggered and square arrays are shown in Figure 9 as a function of the plan area index. For each array geometry, the skin friction is seen to increase monotonically for low values of the obstacle density, corresponding roughly to the isolated flow regime. The skin friction increases with λ_p to a broad maximum that appears to occur for λ_p between about 20 and 30 percent. This range for λ_p corresponds roughly to the wake interference regime. Beyond $\lambda_p \approx 30$ percent, the skin friction decreases and appears to approach an approximately constant value for $\lambda_p \gtrsim 40$ percent, a range which can be associated with the skimming flow regime whereby the obstacles are so closely packed that flow aloft does not penetrate into the obstacle array and a virtually stagnant mean flow is present within the array.

Using the values for α and $u_*/U(h_c)$ provided by Figures 8 and 9 as input to the analytical model, Figure 10 shows the model profiles for k for a square array of cubical obstacles with the plan area index between about 0.05 and 0.20. As expected, the model predicts the increasing attenuation of k with canopy depth as the obstacle density (or, equivalently, as the plan area index) increases. Figures 11 and 12 exhibit model predictions for σ_u and σ_w , respectively, obtained by the equilibrium partitioning of the TKE profiles in Figure 10. As a comparison, Figures 13 and 14 show the model profiles for σ_u and σ_w , respectively, obtained by the algebraic stress model partitioning of the TKE profiles. The data points in Figures 11

and 13 for σ_u/u_* were extracted from Figure 19 of Macdonald et al. [21]. However, the scale used by Macdonald et al. [21] for their Figure 19 only permitted certain values of σ_u/u_* at $\lambda_p = 4.9\%$ and 20% to be extracted unambiguously; in consequence, we have shown only the range in the measured σ_u/u_* data for $\lambda_p \in [4.9, 20]\%$, as the individual data points at the various plan area indices cannot be distinguished unambiguously in Figure 19 of Macdonald et al. [21]. Although the model profiles for the turbulent velocity standard deviations appear to be similar for the equilibrium and algebraic stress model partitioning, a comparison of Figures 11 and 13 seems to suggest that the latter partitioning provides a slightly better reproduction for the range of variation in the σ_u observations.

Macdonald et al. [21] noted that the exponential wind profile does not provide good fits to the observations of within canopy mean wind speed for $\lambda_p \gtrsim 20$ percent. Indeed, for $\lambda_p \gtrsim 40$ percent, the obstacle packing densities are high enough to produce skimming flow implying a near stagnant flow within the obstacle array with a mean wind speed of near zero. We do not expect the analytical model to be valid at these high obstacle packing densities. Nevertheless, we applied the model to obstacle arrays with high packing densities. A comparison of observed and modeled streamwise turbulent velocity standard deviations for $\lambda_p = 69\%$ and 91% are displayed in Figures 15 and 16, for equilibrium and algebraic stress model partitioning of the TKE, respectively. Although the model profile underpredicts σ_u for $\lambda_p = 69\%$, the prediction for $\lambda_p = 91\%$ surprisingly seems to provide a fairly good representation for the observed profile, especially deep in the canopy where σ_u appears to be constant (approximately or better).

Conclusions

In this paper, we describe a fully analytical model for the prediction of the one-dimensional mean wind speed, kinematic shear stress, turbulence kinetic energy, and velocity variances in a horizontally homogeneous canopy. The basis of the model centers around an analytical solution obtained by Massman and Weil [7] for the turbulence kinetic energy derived from a particular form of a second-order closure model for canopy flows developed by Wilson and Shaw [8]. Using this analytical model for the TKE, we showed how to derive analytical expressions for the within canopy velocity variances using two methods: namely, (1) equilibrium partitioning; and, (2) algebraic stress model partitioning derived from an algebraic stress model version of an existing second-order closure model for flows proposed by Launder, Reece, and Rodi [9] that has been modified to include the extra physics arising from the interaction of the airflow with the obstacles in the array.

The analytical model predictions have been compared with some measurements of mean flow and turbulence statistics obtained in two urban canopies: namely, (1) Tombstone canopy; and, (2) arrays of regularly spaced cubical obstacles at various plan area indices. It is shown that the model is moderately successful at providing estimates of a number of important flow quantities; namely, mean wind speed and various turbulence statistics. Given the limited data that was available, we have been unable to ascertain whether the algebraic stress model partitioning of the TKE offers any significant advantages in the determination of the velocity variances over the simpler equilibrium partitioning. Certainly, the measured profiles for σ_u appear to be different in shape than those of σ_w (viz., there appear to be differences in the concavity of the σ_u and σ_w profiles), a general behavior that can be captured potentially by the algebraic stress model partitioning but not by the equilibrium partitioning of the TKE. The assumption of an exponential wind profile may not be valid for urban arrays at high plan area indices where the skimming flow regime is dominant and a virtually stagnant flow is found within the urban array. However, even under these extreme conditions, the analytical model has been found to provide a fairly good approximation for the profiles of the turbulence statistics. On the positive side, the analytical model described herein affords a relatively simple method for the prediction of canopy flows (both mean wind and turbulence statistics) and appears to capture enough of the salient qualitative features of these flows to be useful. With the testing of the analytical model against the urban canopy flows and its modest success, it is suggested that this analytical model for canopy flows can probably be applied unmodified to a wide range of canopies, both vegetative and urban. Experience seems to indicate that this imperfect model may give adequate solutions for certain applications.

The one-dimensional analytical model for canopy flows considered in this report provides all the statistics of the wind field (mean wind speed, kinematic shear stress, velocity variances, and viscous dissipation rate) required as input to drive a physically-based model for the prediction of urban dispersion. These flow statistics can be calculated rapidly using the analytical model in comparison to the more computationally intensive second-order closure models for canopy flows. Taken as a whole, this simple canopy flow model can probably be used to "drive" a Lagrangian stochastic dispersion model for the prediction of dispersion of materials released within a canopy. The next logical step in this work would be to construct a Lagrangian stochastic model satisfying the well-mixed criterion that uses the simple analytical model to provide the input mean flow and turbulence quantities required.

References

1. Inoue, E. (1963). On the Turbulent Structure of Airflow Within Crop Canopies, *J. Meteorol. Soc. Japan*, 41, 317–326.
2. Cionco, R. M. (1965). A Mathematical Model for Air Flow in a Vegetative Canopy. *J. Appl. Meteorol.*, 4, 517–522.
3. Cionco, R. M. (1972). A Wind Profile Index for Canopy Flow. *Boundary-Layer Meteorol.*, 3, 225–263.
4. Massman, W. J. (1997). An Analytical One-Dimensional Model of Momentum Transfer by Vegetation of Arbitrary Structure. *Boundary-Layer Meteorol.*, 83, 407–421.
5. Thom, A.S. (1971). Momentum Absorption by Vegetation. *Quart. J. Roy. Meteorol. Soc.*, 97, 414–428.
6. Jackson, P. S. (1981). On the Displacement Height in the Logarithmic Velocity Profile. *J. Fluid Mech.*, 111, 15–25.
7. Massman, W. J. and Weil, J. C. (1999). An Analytical One-Dimensional Second-Order Closure Model of Turbulence Statistics and the Lagrangian Time Scale Within and Above Plant Canopies of Arbitrary Structure. *Boundary-Layer Meteorol.* 91, 81–107.
8. Wilson, N. R. and Shaw, R. H. (1977). A Higher-Order Closure Model for Canopy Flow. *J. Appl. Meteorol.*, 16, 1197–1205.
9. Launder, B. E., Reece, G. T., and Rodi, W. (1975). The Development of a Reynolds Stress Turbulent Closure. *J. Fluid Mech.*, 68, 537–566.
10. Wilson, J. D., Finnigan, J. J., and Raupach, M. R. (1998). A First-Order Closure for Disturbed Plant-Canopy Flows, and Its Application to Winds in a Canopy on a Ridge. *Q. J. R. Meteorol. Soc.*, 124, 705–732.
11. Raupach, M. R., Finnigan, J. J., and Brunet, Y. (1996). Coherent Eddies and Turbulence in Vegetation Canopies: The Mixing-Layer Analogy. *Boundary-Layer Meteorol.*, 78, 351–382.
12. Townsend, A. A. (1976). *The Structure of Turbulent Shear Flow*, Second Edition, Cambridge University Press, Cambridge, England.
13. Raupach, M. R. (1992). Drag and Drag Partition on Rough Surfaces. *Boundary-Layer Meteorol.*, 60, 375–395.

14. Raupach, M. R. (1994). Simplified Expressions for Vegetation Roughness Length and Zero-Plane Displacement as Functions of Canopy Height and Area Index. *Boundary-Layer Meteorol.*, 71, 211–216.
15. Hanna, S. R. and Britter, R. E. (2000). *The Effect of Roughness Obstacles on Flow and Dispersion at Industrial Facilities*, CCPS Project 132, Vapor Cloud Subcommittee, CCPS/AIChE, New York.
16. Macdonald, R. W., Griffiths, R. F., and Hall, D. J. (1998). An Improved Method for Estimation of Surface Roughness of Obstacle Arrays. *Atmos. Environ.*, 32, 1857–1864.
17. Duijm, N. J. (1999). Estimates of Roughness Parameters for Arrays of Obstacles. *Boundary-Layer Meteorol.*, 91, 1–22.
18. Bottema, M. (1996). Roughness Parameters Over Regular Rough Surfaces: Experimental Requirements and Model Validation. *J. Wind Eng. Ind. Aerodyn.* 64, 249–265.
19. Bottema, M. (1997). Urban Roughness Modeling in Relation to Pollutant Dispersion. *Atmos. Environ.*, 31, 3059–3075.
20. Grimmond, C. S. B. and Oke, T. R. (1999). Aerodynamic Properties of Urban Areas Derived from Analysis of Surface Form. *J. Appl. Meteorol.* 38, 1262–1292.
21. Macdonald, R. W., Hall, D. J., Walker, S., and Spanton, A. M. (1998). *Wind Tunnel Measurements of Windspeed Within Simulated Urban Arrays*, BRE CR 243/98, Building Research Establishment, Garston, Watford, UK.
22. Shaw, R. H., Silversides, R. H., and Thurtell, G. W. (1974). Some Observations of Turbulence and Turbulent Transport within and above Plant Canopies. *Boundary-Layer Meteorol.*, 5, 429–449.
23. Wilson, J. D., Ward, D. P., Thurtell, G. W., and Kidd, G. E. (1982). Statistics of Atmospheric Turbulence Within and Above a Corn Canopy. *Boundary-Layer Meteorol.*, 24, 495–519.
24. Amiro, B. D. (1990). Comparison of Turbulence Statistics within Three Boreal Forest Canopies. *Boundary-Layer Meteorol.*, 51, 99–121.
25. Lee, Y. and Black, T. A. (1993). Atmospheric Turbulence Within and Above a Douglas-Fir Stand. Part I: Statistical Properties of the Vertical Velocity Field. *Boundary-Layer Meteorol.*, 64, 149–174.
26. Katul, G. G. and Albertson, J. D. (1998). An Investigation of Higher Order Closure Models for a Forested Canopy. *Boundary-Layer Meteorol.*, 89, 47–74.

27. Brunet, Y., Finnigan, J. J., and Raupach, M. R. (1994). A Wind Tunnel Study of Air Flow in Waving Wheat: Single-Point Statistics. *Boundary-Layer Meteorol.*, 70, 95-132.
28. Raupach, M. R., Coppin, P. A., and Legg, B. J. (1986). Experiments on Scalar Dispersion Within a Model Plant Canopy, Part I: The Turbulence Structure. *Boundary-Layer Meteorol.*, 35, 21-52.

This page intentionally left blank

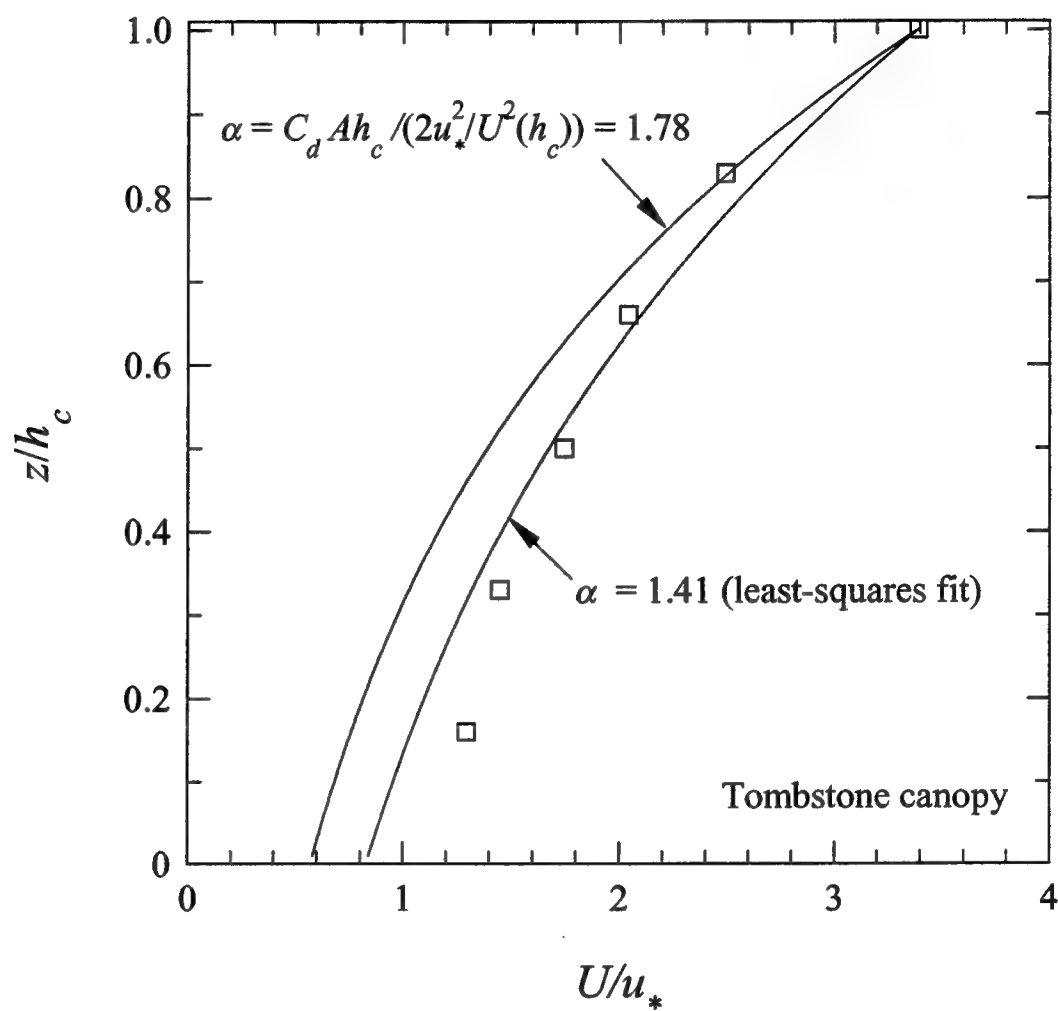


Figure 1. Comparison of the observed profile of the mean wind speed (open squares) in the Tombstone canopy with model prediction.

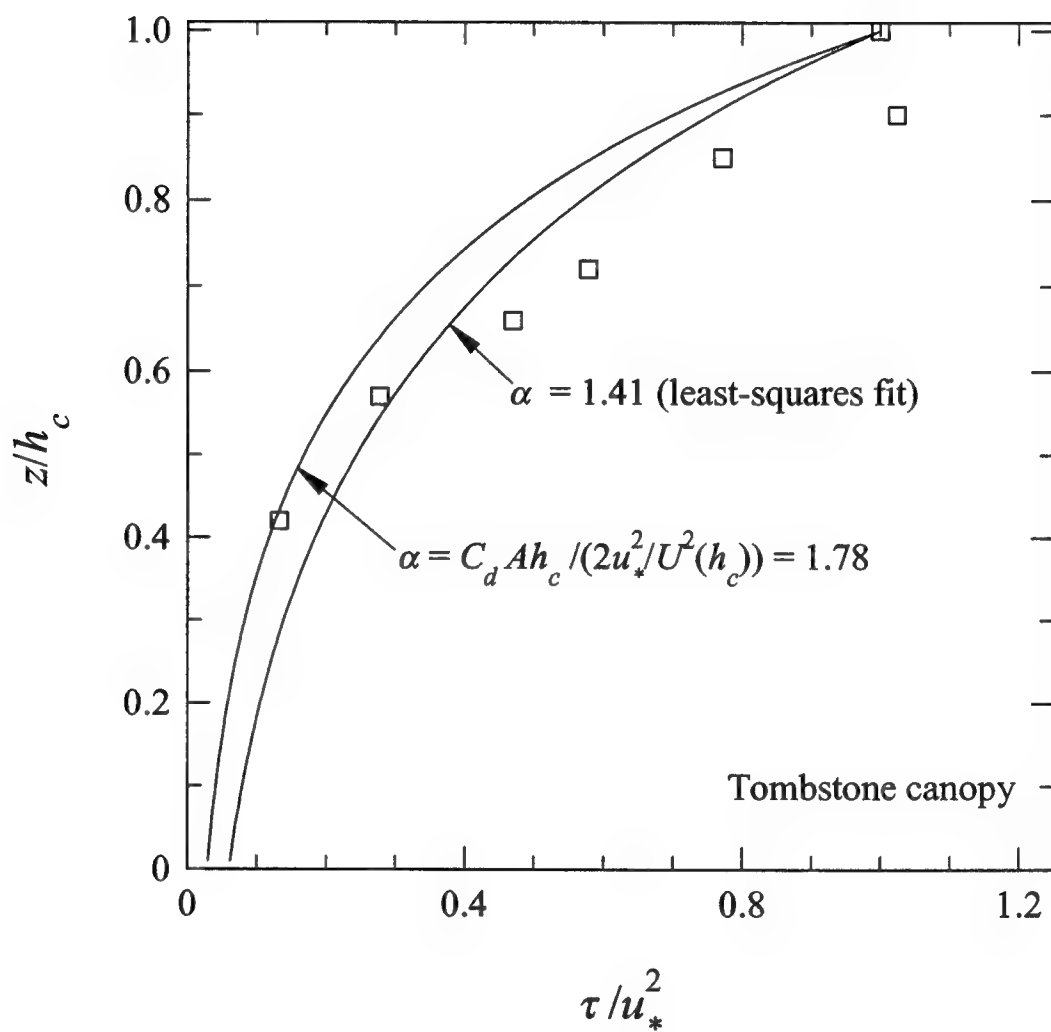


Figure 2. Comparison of the observed profile of the kinematic shear stress (open squares) in the Tombstone canopy with model predictions.

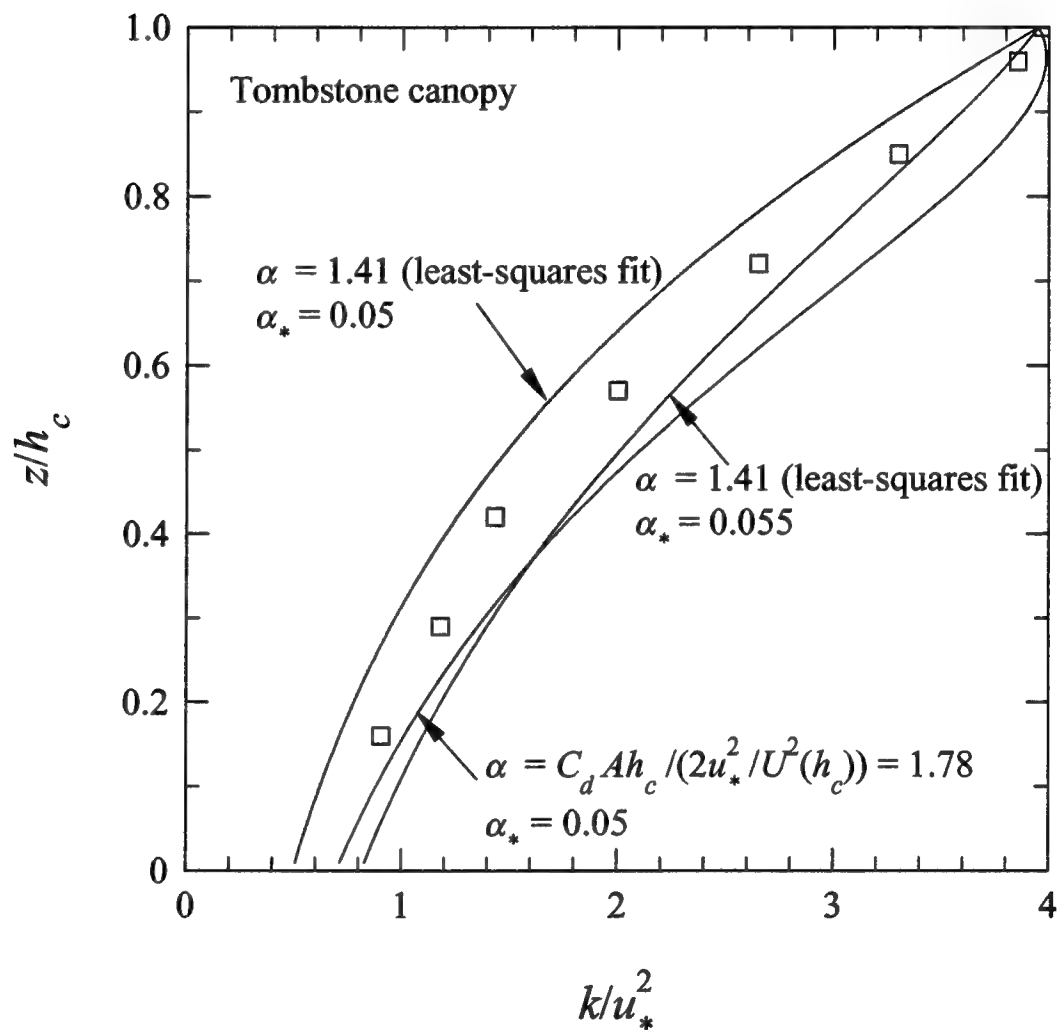


Figure 3. Comparison of the observed profile of the turbulence kinetic energy (open squares) in the Tombstone canopy with model prediction.

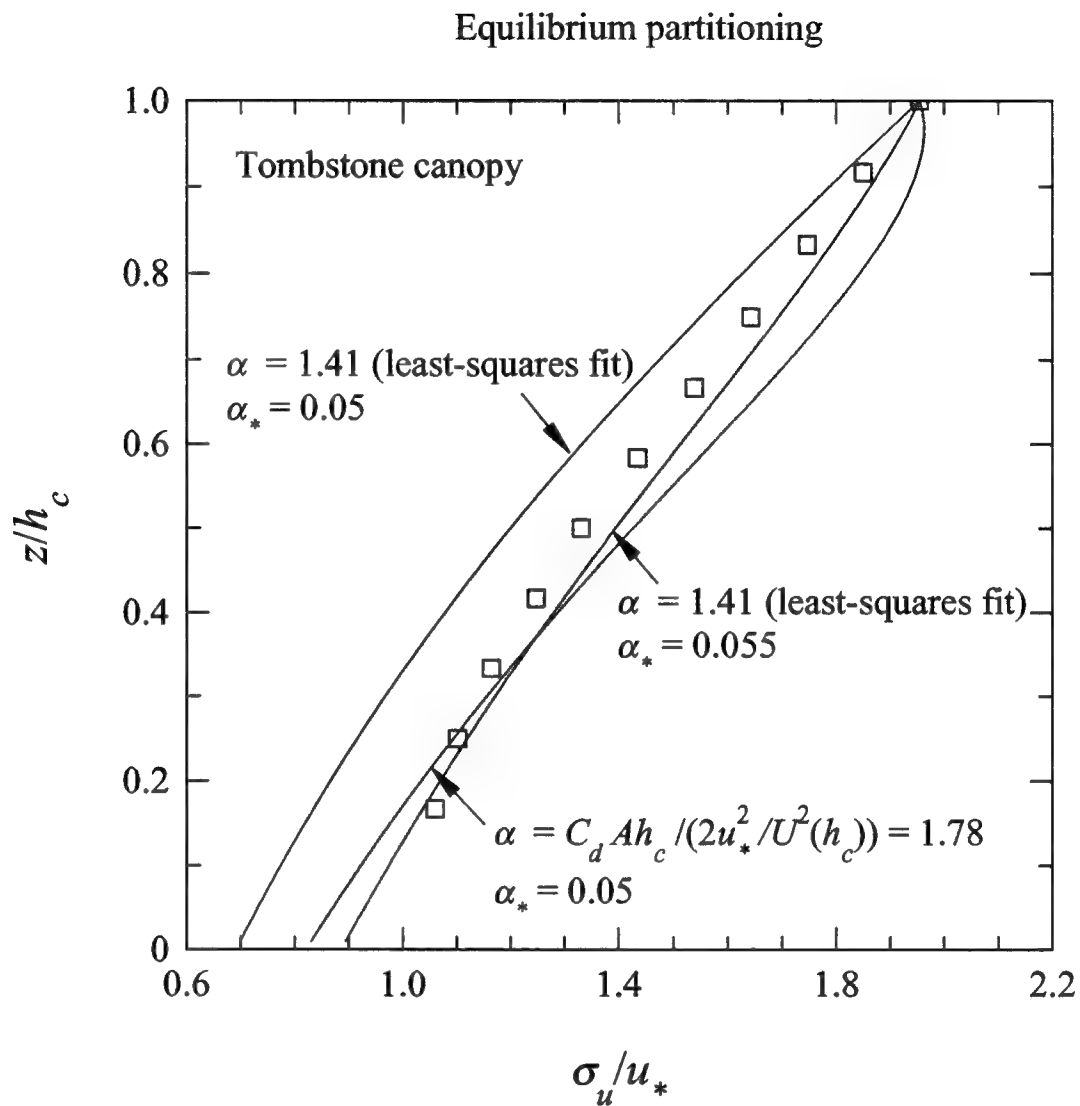


Figure 4. Comparison of the observed profile of the streamwise turbulent velocity standard deviation (open squares) in the Tombstone canopy with model prediction obtained by equilibrium partitioning of the turbulence kinetic energy.

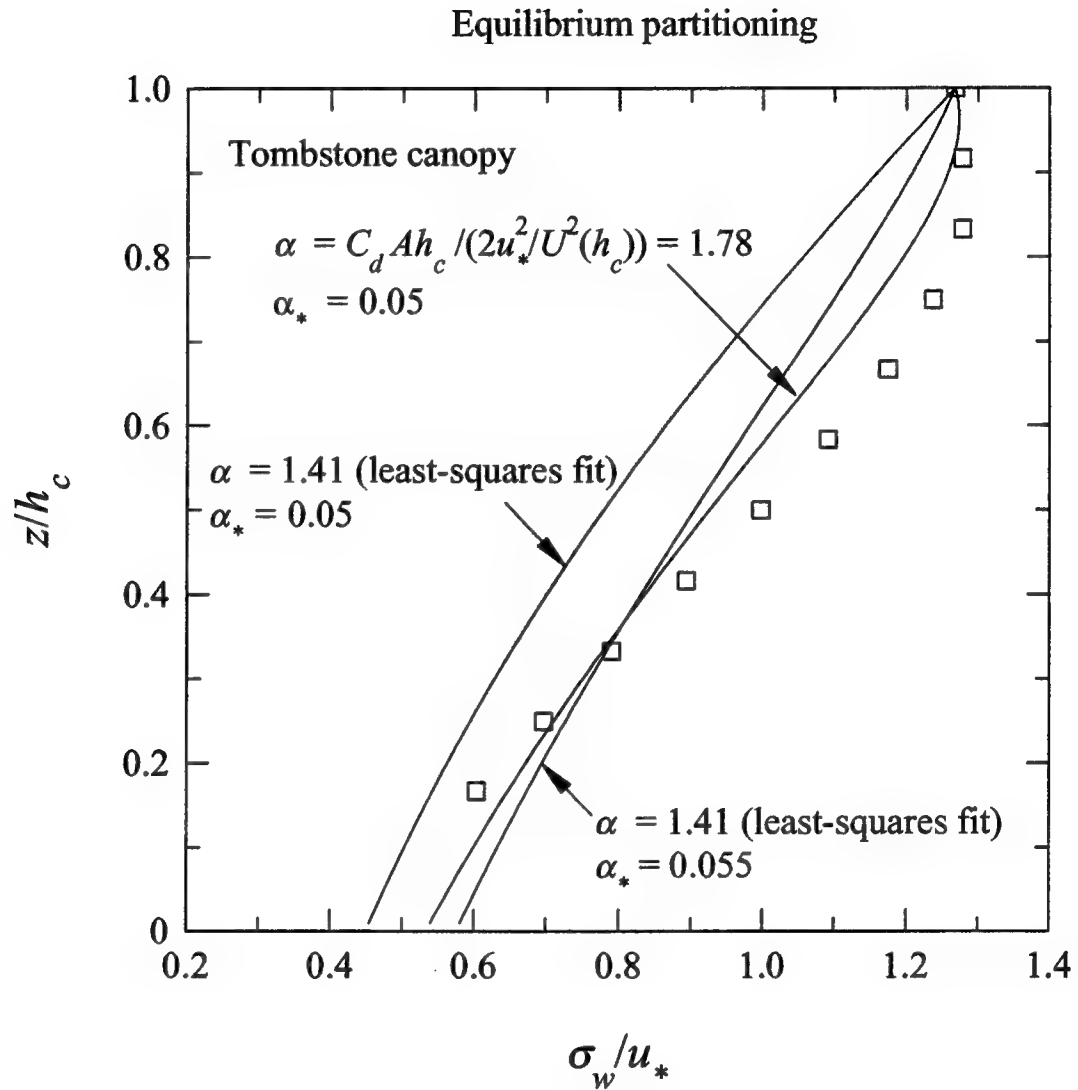


Figure 5. Comparison of the observed profile of the vertical turbulent velocity standard deviation (open squares) in the Tombstone canopy with model prediction obtained by equilibrium partitioning of the turbulence kinetic energy.

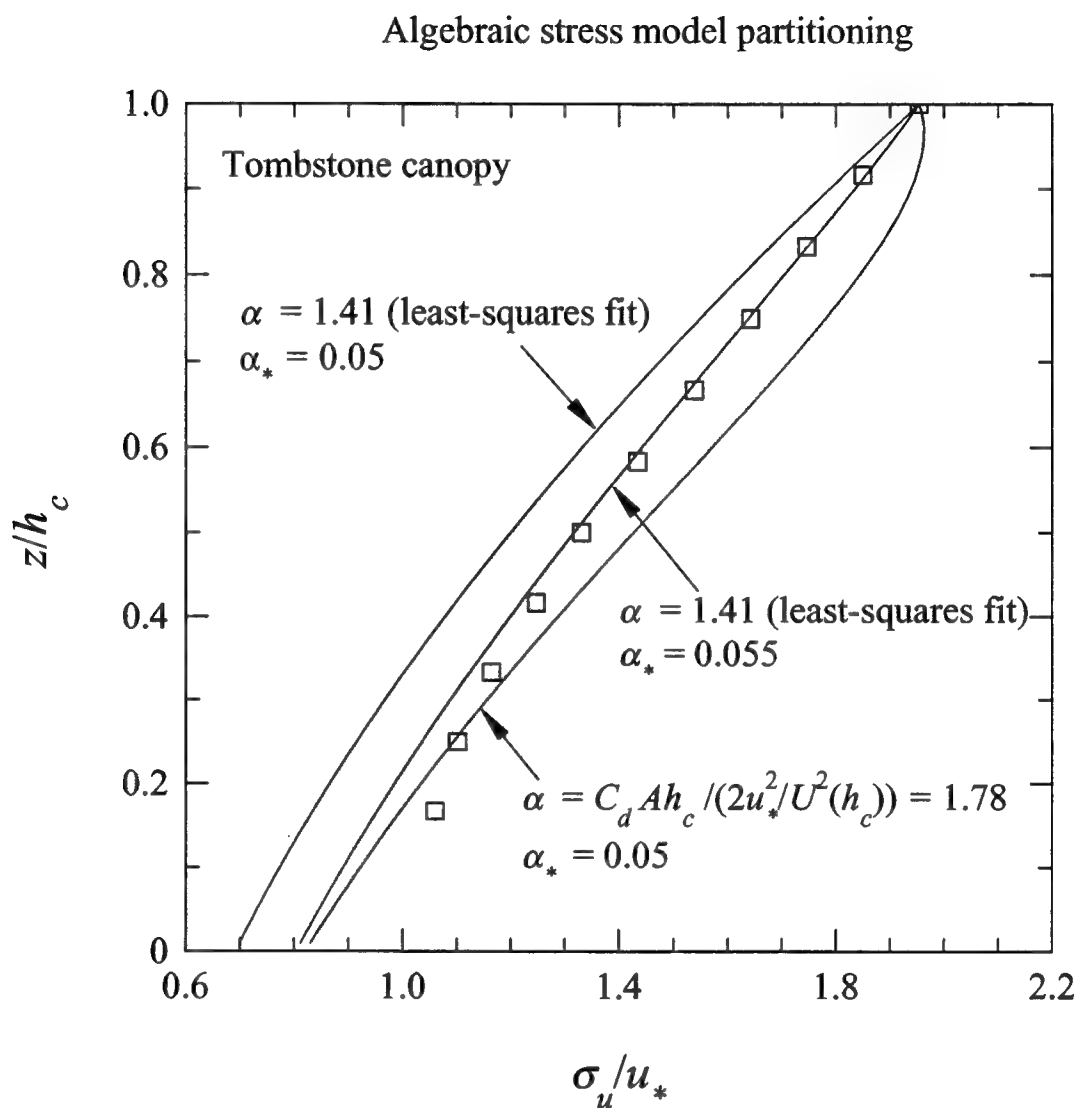


Figure 6. Comparison of the observed profile of the streamwise turbulent velocity standard deviation (open squares) in the Tombstone canopy with model prediction obtained by algebraic stress model partitioning of the turbulence kinetic energy.

Algebraic stress model partitioning

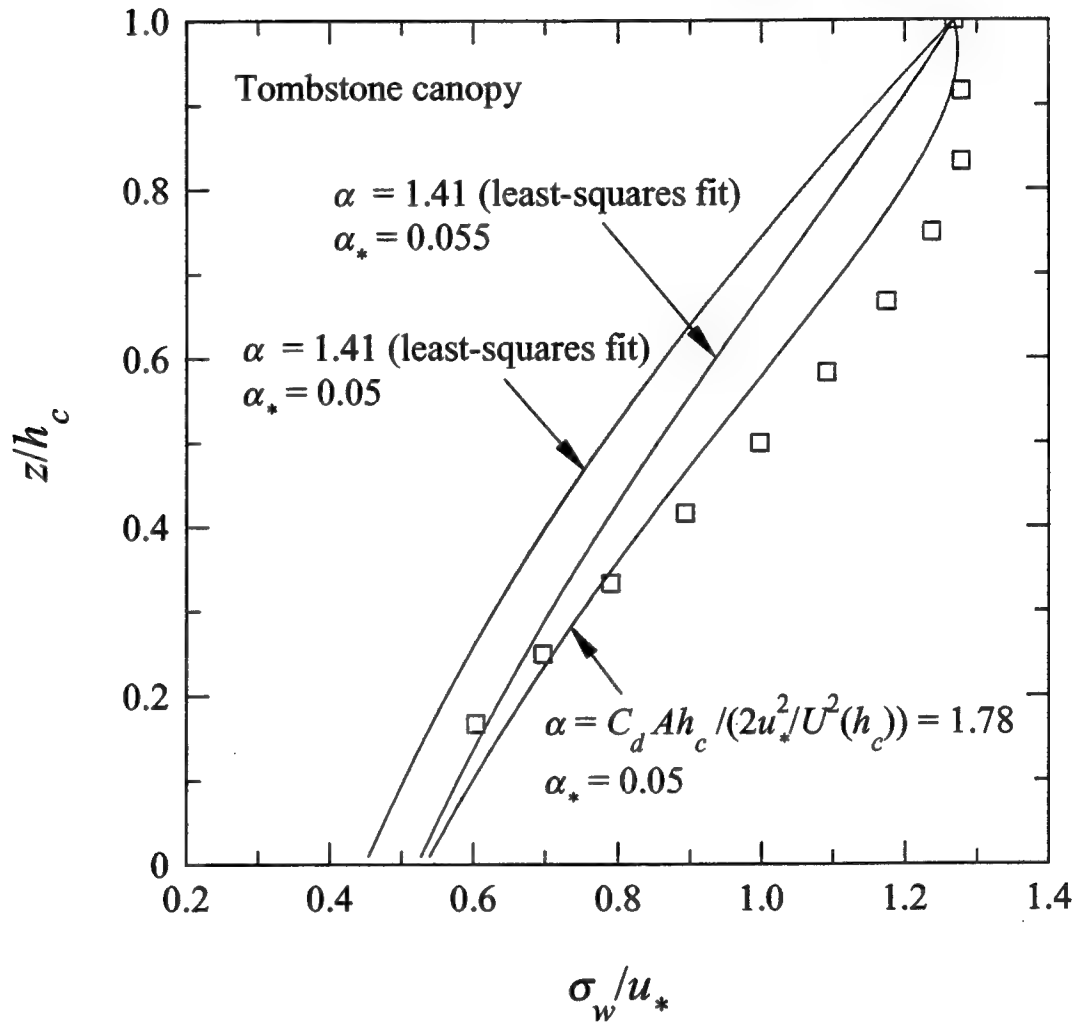


Figure 7. Comparison of the observed profile of the vertical turbulent velocity standard deviation (open squares) in the Tombstone canopy with model prediction obtained by algebraic stress model partitioning of the turbulence kinetic energy.

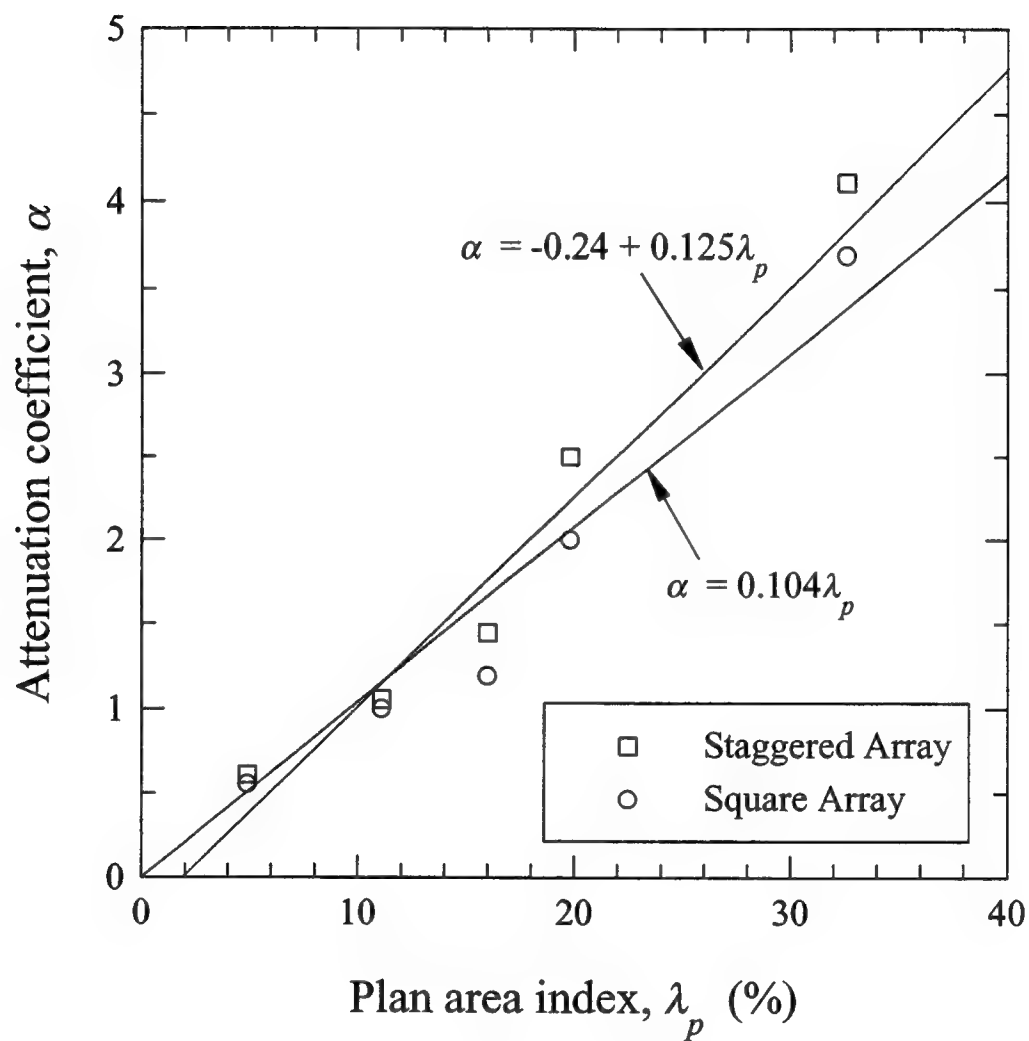


Figure 8. Comparison of the observed values of the attenuation coefficient at various plan area indices for staggered and square arrays of cubical obstacles with two proposed parameterizations.

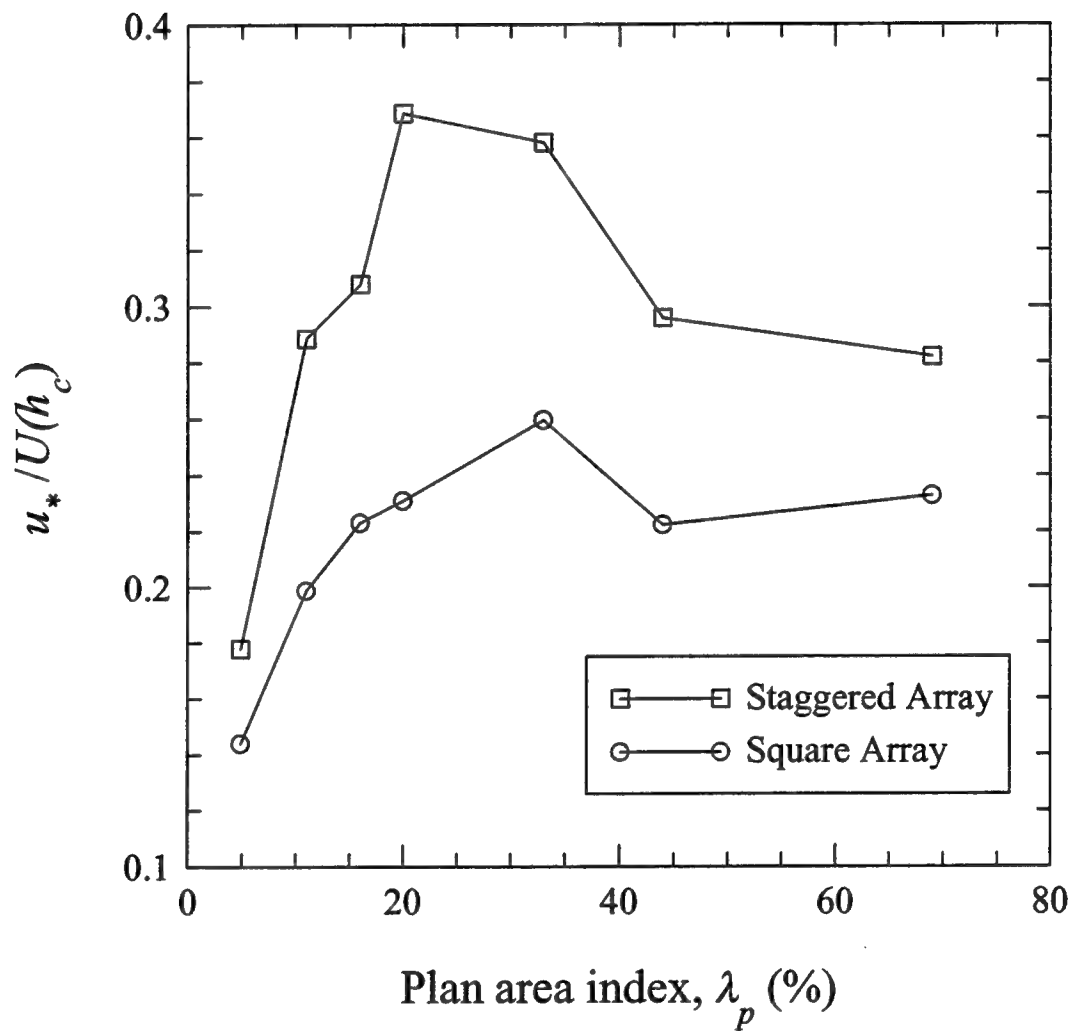


Figure 9. The observed variation of the skin friction at canopy height as a function of the plan area index for staggered and square arrays of cubical obstacles.

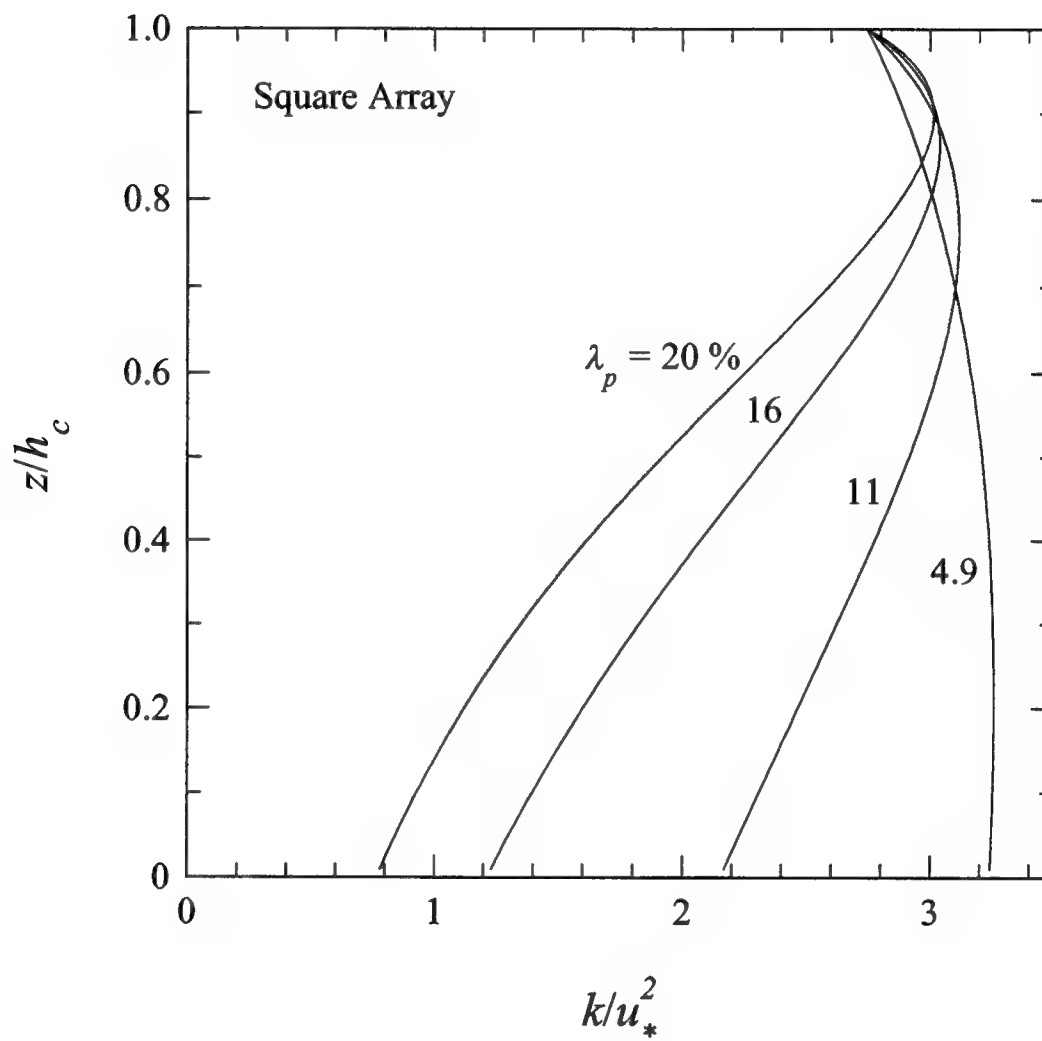


Figure 10. Model predictions of profiles of the turbulence kinetic energy for a square array of cubical obstacles with various plan area indices.

Equilibrium partitioning

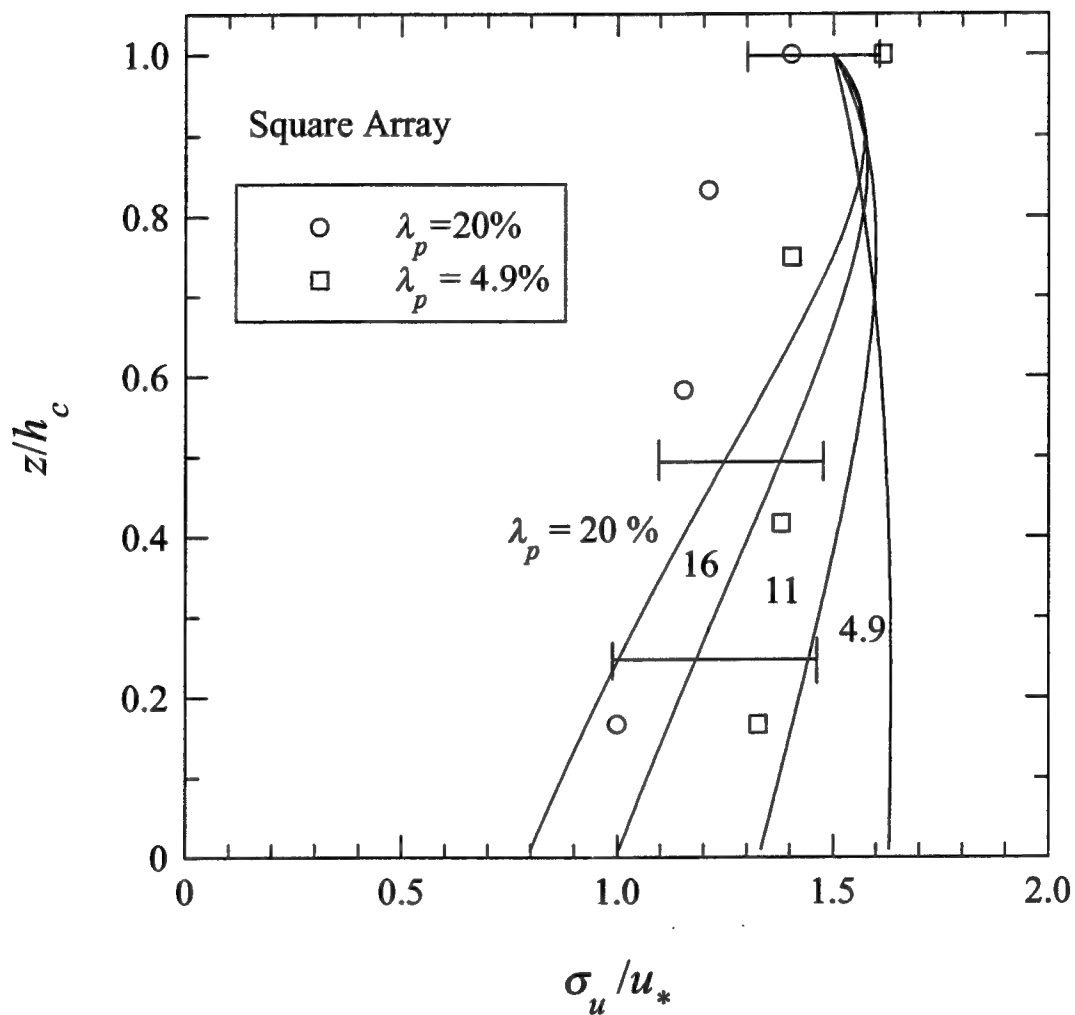


Figure 11. Model predictions of profiles of streamwise turbulent velocity standard deviation for a square array of cubical obstacles with various plan area indices. The modeled profiles were obtained using equilibrium partitioning of the turbulence kinetic energy. The horizontal bars show the range in the observations by Macdonald et al. [21].

Equilibrium partitioning

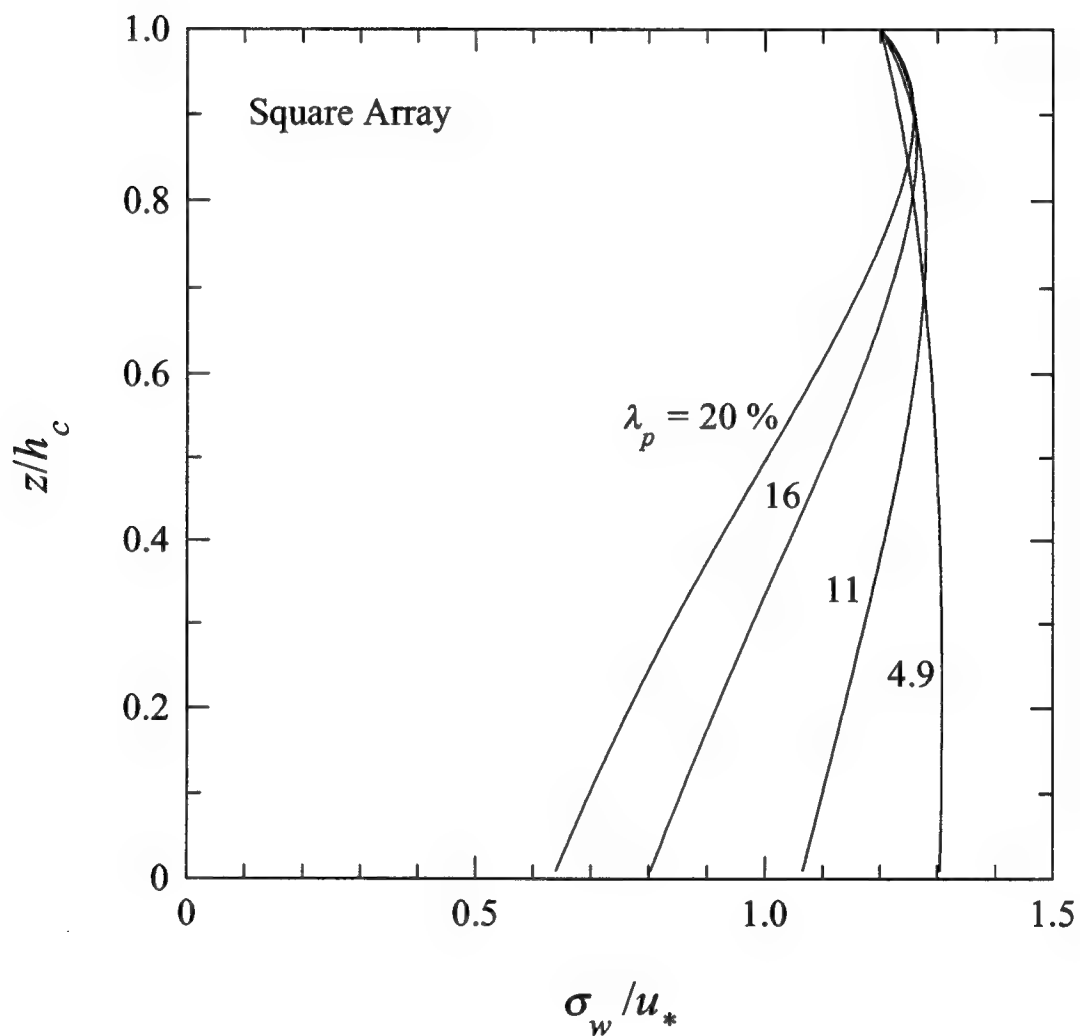


Figure 12. Model predictions of profiles of vertical turbulent velocity standard deviation for a square array of cubical obstacles with various plan area indices. The modeled profiles were obtained using equilibrium partitioning of the turbulence kinetic energy.

Algebraic stress model partitioning

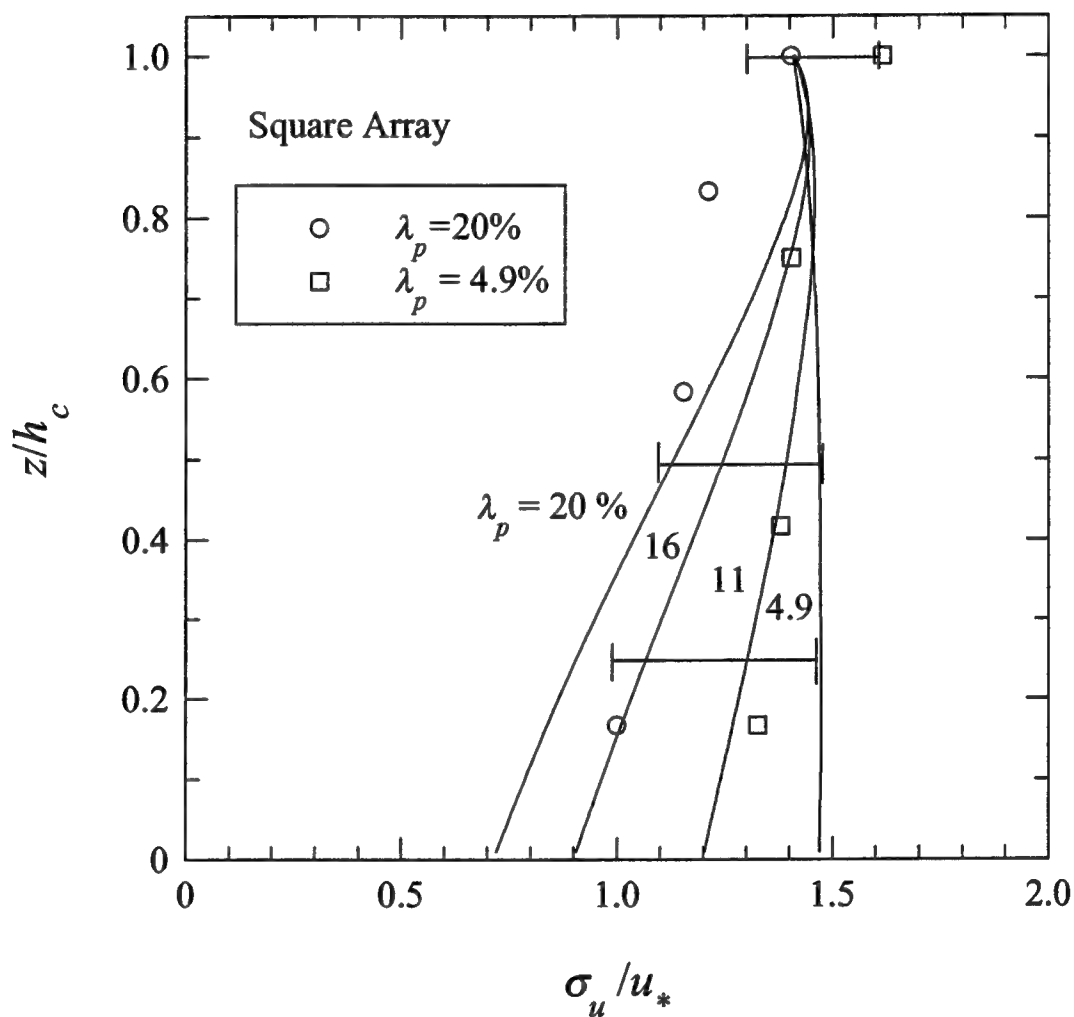


Figure 13. Model predictions of profiles of streamwise turbulent velocity standard deviation for a square array of cubical obstacles with various plan area indices. The modeled profiles were obtained using algebraic stress model partitioning of the turbulence kinetic energy. The horizontal bars show the range in the observations by Macdonald et al. [21].

Algebraic stress model partitioning

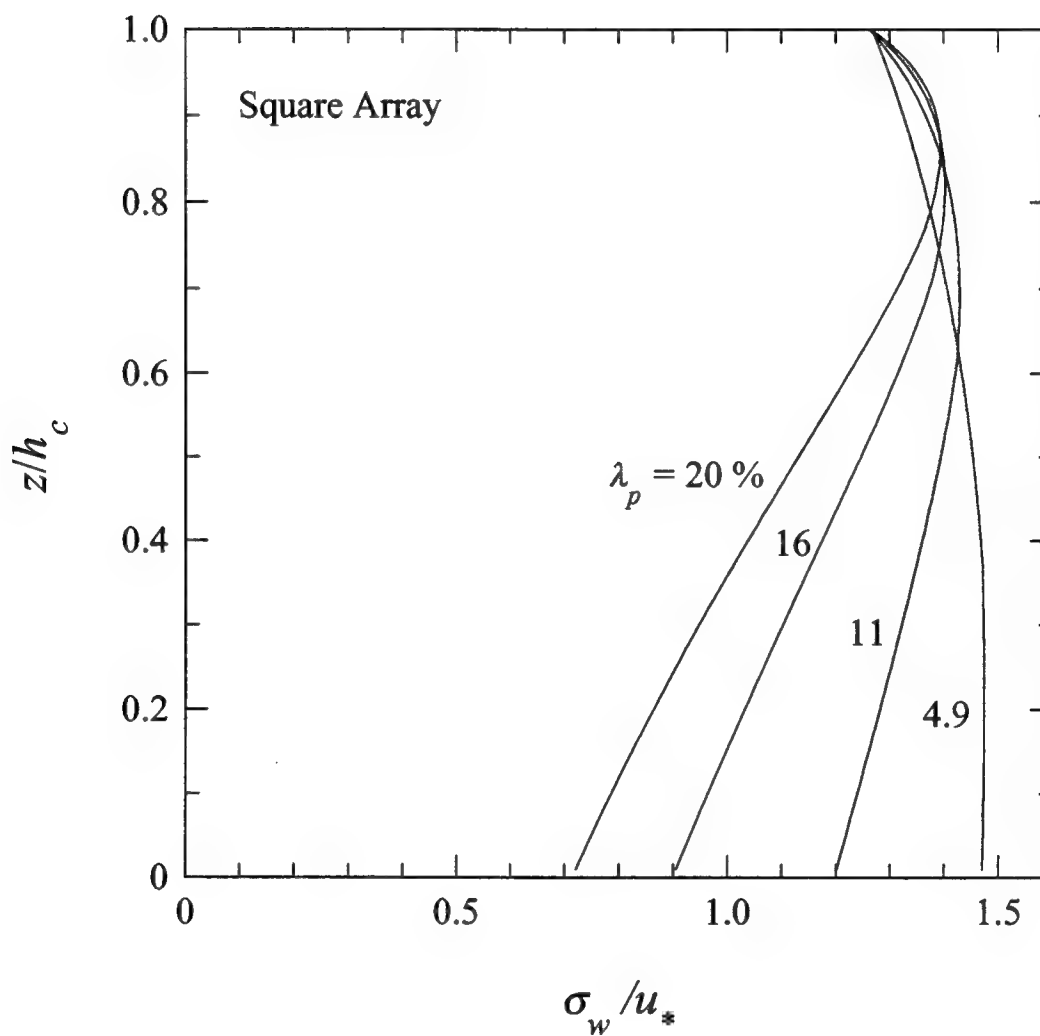


Figure 14. Model predictions of profiles of vertical turbulent velocity standard deviation for a square array of cubical obstacles with various plan area indices. The modeled profiles were obtained using algebraic stress model partitioning of the turbulence kinetic energy.

Equilibrium partitioning

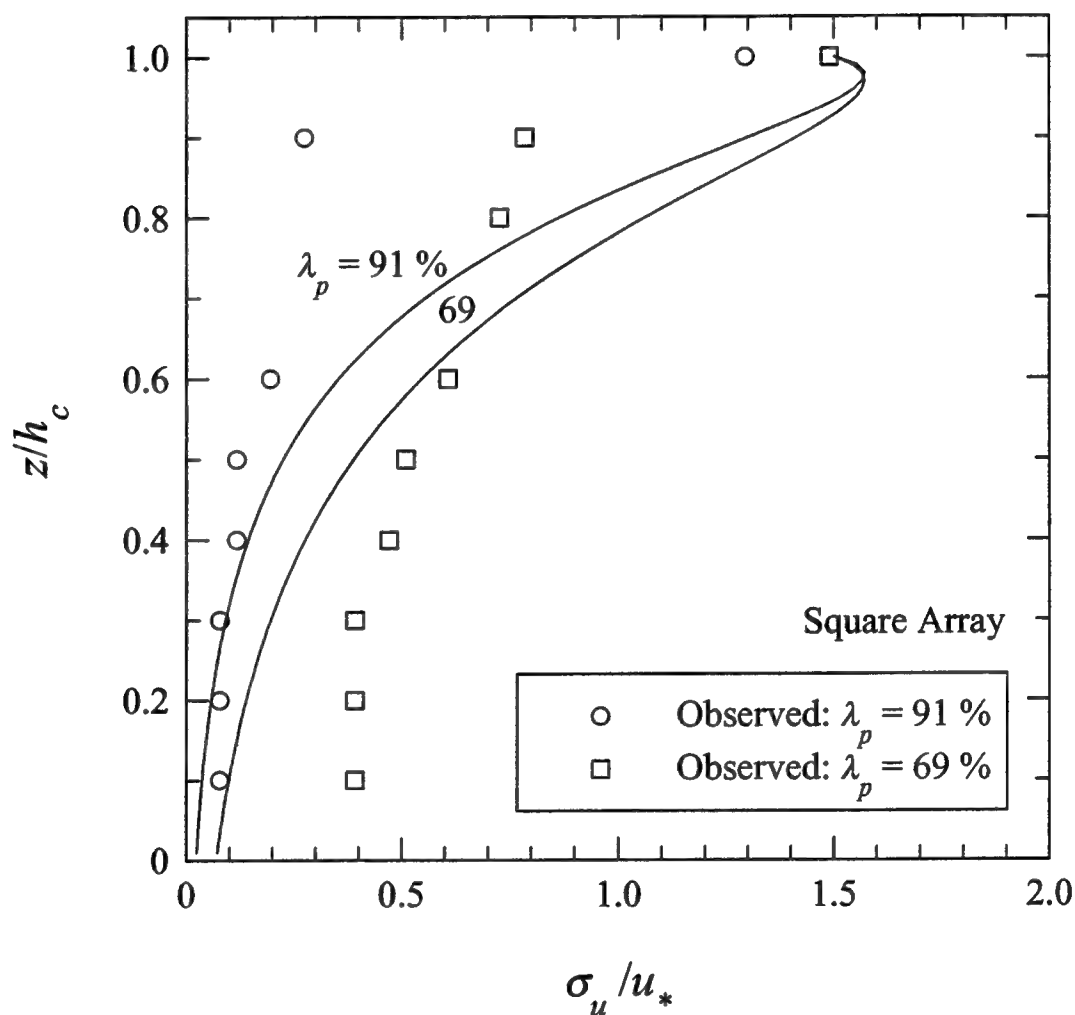


Figure 15. Model predictions of profiles of streamwise turbulent velocity standard deviation for a square array of cubical obstacles at high plan area indices. The modeled profiles were obtained using equilibrium partitioning of the turbulence kinetic energy. Open symbols are measurements made by Macdonald et al. [21].

Algebraic stress model partitioning

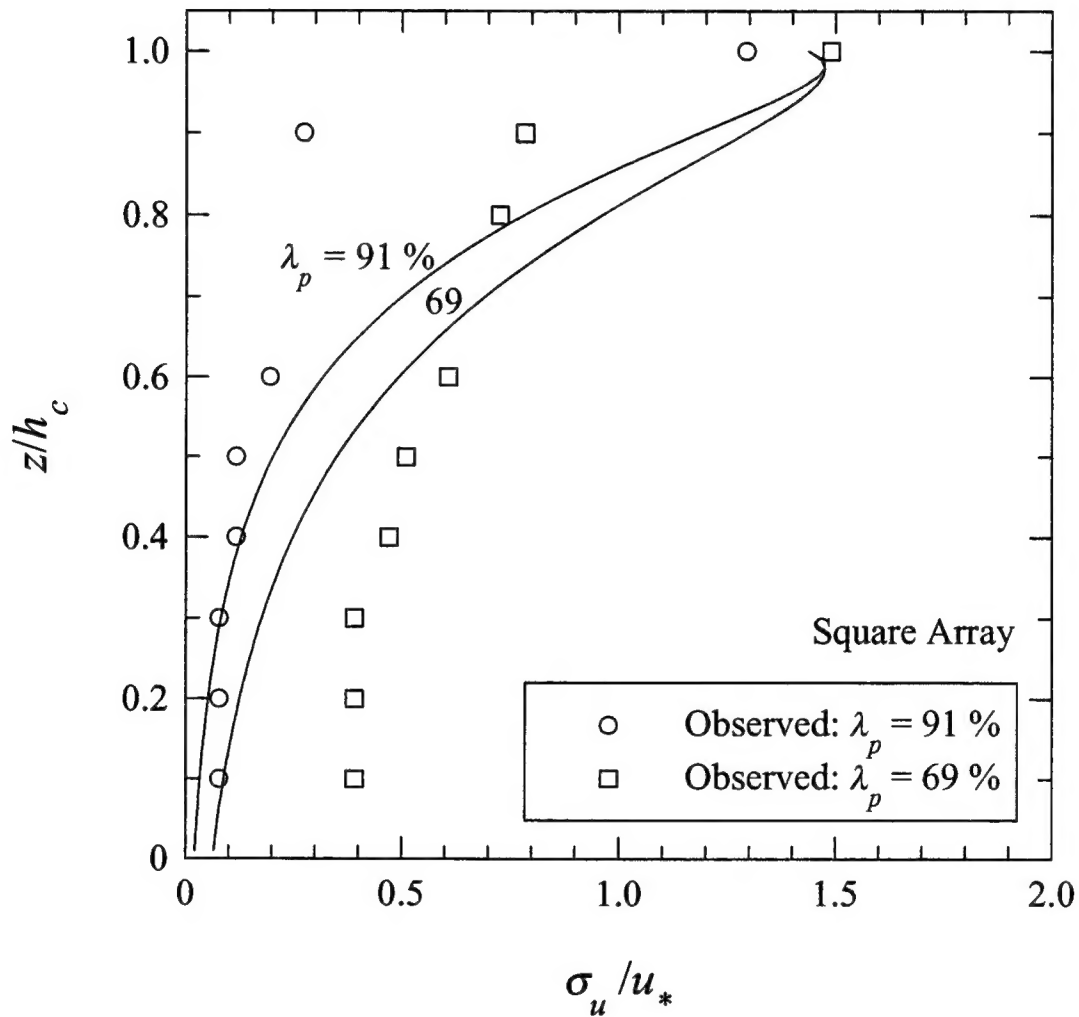


Figure 16. Model predictions of profiles of streamwise turbulent velocity standard deviation for a square array of cubical obstacles at high plan area indices. The modeled profiles were obtained using algebraic stress model partitioning of the turbulence kinetic energy. Open symbols are measurements made by Macdonald et al. [21].

UNCLASSIFIED

SECURITY CLASSIFICATION OF FORM
(highest classification of Title, Abstract, Keywords)

DOCUMENT CONTROL DATA

(Security classification of title, body of abstract and indexing annotation must be entered when the overall document is classified)

1. ORIGINATOR (the name and address of the organization preparing the document. Organizations for whom the document was prepared, e.g. Establishment sponsoring a contractor's report, or tasking agency, are entered in section 8.) Defence Research Establishment Suffield P.O. Box 4000 Medicine Hat, Alberta T1A 8K6		2. SECURITY CLASSIFICATION (overall security classification of the document including special warning terms if applicable) UNCLASSIFIED	
3. TITLE (the complete document title as indicated on the title page. Its classification should be indicated by the appropriate abbreviation (S,C,R or U) in parentheses after the title.) A One-Dimensional Mean Wind and Turbulence Model for a Uniform Urban Canopy (U)			
4. AUTHORS (last name, first name, middle initial. If military, show rank, e.g. Doe, Maj. John E.) Yee, Eugene C.			
5. DATE OF PUBLICATION (month and year of publication of document) October 2000		6a. NO. OF PAGES (total containing information. Include Annexes, Appendices, etc.) 51	6b. NO. OF REFS (total cited in document) 28
6. DESCRIPTIVE NOTES (the category of the document, e.g. technical report, technical note or memorandum. If appropriate, enter the type of report, e.g. interim, progress, summary, annual or final. Give the inclusive dates when a specific reporting period is covered.) Technical Report (Final) [1 January, 2000 to 30 June, 2000]			
8. SPONSORING ACTIVITY (the name of the department project office or laboratory sponsoring the research and development. Include the address.) Defense Threat Reduction Agency 6801 Telegraph Road Alexandria, VA 22310-3398			
9a. PROJECT OR GRANT NO. (if appropriate, the applicable research and development project or grant number under which the document was written. Please specify whether project or grant) PCN No. 6QD11		9b. CONTRACT NO. (if appropriate, the applicable number under which the document was written)	
10a. ORIGINATOR'S DOCUMENT NUMBER (the official document number by which the document is identified by the originating activity. This number must be unique to this document.) DRES TR 2000-071		10b. OTHER DOCUMENT NOS. (Any other numbers which may be assigned this document either by the originator or by the sponsor)	
11. DOCUMENT AVAILABILITY (any limitations on further dissemination of the document, other than those imposed by security classification) <input checked="" type="checkbox"/> Unlimited distribution <input type="checkbox"/> Distribution limited to defence departments and defence contractors; further distribution only as approved <input type="checkbox"/> Distribution limited to defence departments and Canadian defence contractors; further distribution only as approved <input type="checkbox"/> Distribution limited to government departments and agencies; further distribution only as approved <input type="checkbox"/> Distribution limited to defence departments; further distribution only as approved <input type="checkbox"/> Other (please specify):			
12. DOCUMENT ANNOUNCEMENT (any limitation to the bibliographic announcement of this document. This will normally correspond to the Document Availability (11). However, where further distribution (beyond the audience specified in 11) is possible, a wider announcement audience may be selected.) No			

UNCLASSIFIED

SECURITY CLASSIFICATION OF FORM

UNCLASSIFIED

SECURITY CLASSIFICATION OF FORM

13. **ABSTRACT** (a brief and factual summary of the document. It may also appear elsewhere in the body of the document itself. It is highly desirable that the abstract of classified documents be unclassified. Each paragraph of the abstract shall begin with an indication of the security classification of the information in the paragraph (unless the document itself is unclassified) represented as (S), (C), (R), or (U). It is not necessary to include here abstracts in both official languages unless the text is bilingual).

A fully analytical model for the prediction of the one-dimensional mean wind speed, kinematic shear stress, turbulence kinetic energy, and velocity variances in a horizontally homogeneous canopy is described. The basis of the model centers around an analytical solution obtained by Massman and Weil (Boundary-Layer Meteorology, 91, pp. 81-107, 1999) for the turbulence kinetic energy derived from a particular form of a second-order closure model for canopy flows. Using this analytical model for the turbulence kinetic energy, it is shown how to derive analytical expressions for the within canopy velocity variances using two methods: namely, (1) equilibrium partitioning whereby the velocity variances are assumed to be proportional to the turbulence kinetic energy, with the proportionality constants the same as those at the canopy top; and, (2) algebraic stress model partitioning derived from an algebraic stress model version of an existing second-order closure model for flows proposed by Launder, Reece, and Rodi (Journal of Fluid Mechanics, 68, pp. 537-566, 1975) that has been modified to include the effects on the turbulence of the extra physics arising from the interaction of the airflow with the obstacles in the array (viz., the form drag on the canopy elements, and the role of the momentum absorption over an extended volume of space on the turbulent motions within the canopy).

The predictions from the analytical model have been compared with some measurements of mean flow and turbulence statistics obtained in two urban canopies; namely, (1) Tombstone canopy; and, (2) arrays of regularly spaced cubical obstacles at various plan area indices. It is shown that the model is moderately successful at providing estimates of a number of important flow quantities; namely, mean wind speed and various turbulence statistics. Given the limited data that was available, it has not been possible to ascertain whether the algebraic stress model partitioning of the turbulence kinetic energy offers any significant advantages in the determination of the component velocity variances over the simpler equilibrium partitioning. With the testing of the analytical model against the urban canopy flows and its modest success, it is suggested that this analytical model for canopy flows can probably be applied unmodified to a wide range of canopies, both vegetative and urban.

14. **KEYWORDS, DESCRIPTORS or IDENTIFIERS** (technically meaningful terms or short phrases that characterize a document and could be helpful in cataloguing the document. They should be selected so that no security classification is required. Identifiers, such as equipment model designation, trade name, military project code name, geographic location may also be included. If possible keywords should be selected from a published thesaurus. e.g. Thesaurus of Engineering and Scientific Terms (TEST) and that thesaurus-identified. If it is not possible to select indexing terms which are Unclassified, the classification of each should be indicated as with the title.)

Urban Flow Modeling
Turbulence Modeling in Urban Canopies
Analytical Models of Wind Flow

UNCLASSIFIED

SECURITY CLASSIFICATION OF FORM

The Defence Research
and Development Branch
provides Science and
Technology leadership
in the advancement and
maintenance of Canada's
defence capabilities.

Leader en sciences et
technologie de la défense,
la Direction de la recherche
et du développement pour
la défense contribue
à maintenir et à
accroître les compétences
du Canada dans
ce domaine.



www.crad.dnd.ca

